

ANALYSIS OF STRIP ANTENNAS IN THE PRESENCE
OF A DIELECTRIC INHOMOGENEITY

Edward H. Newman

TECHNICAL REPORT 2902-20

OCTOBER 1974

Grant NGL 36-003-138

National Aeronautics and Space Administration
Langley Research Center
Hampton, Va. 23365



ABSTRACT

Three moment method solutions are considered for treating the problem of wire antennas in the presence of an arbitrary dielectric inhomogeneity. In the first method, the current on the wire and the electric field intensity in the inhomogeneity are treated as independent unknowns, while in the second and third methods they are treated as dependent unknowns. The third method is applied to the problem of strip antennas in an electrically thin dielectric slab. Numerical results are presented, and are in good agreement with measurements and previous calculations.

ACKNOWLEDGMENTS

The author wishes to express his sincere gratitude to his graduate adviser, Professor J. H. Richmond, for his help and guidance in this work and for his reading of this manuscript. Professor C. H. Walter deserves special thanks for his reading of this manuscript and for many helpful and interesting discussions. Gratitude is also owed to Professor G. A. Thiele and Dr. N. N. Wang for their critical reading of this manuscript.

The material contained in this report is also used as a dissertation submitted to the Department of Electrical Engineering, The Ohio State University as partial fulfillment for the degree Doctor of Philosophy.

CONTENTS

	Page
I INTRODUCTION.....	1
II STRIP ANTENNA IN A HOMOGENEOUS MEDIUM.....	3
III STRIP ANTENNA IN THE PRESENCE OF AN ARBITRARY DIELECTRIC INHOMOGENEITY.....	12
A. Introduction	12
B. Approach 1 - The Wire Current and the Electric Field in the Inhomogeneity are Considered to be Independent Unknowns	13
C. Approach 2 - The Wire Current and The Electric Field in the Inhomogeneity are Considered to be Dependent Unknowns	17
IV STRIP ANTENNA LOCATED IN THE CENTER OF A THIN DIELECTRIC SLAB.....	22
V STRIP ANTENNA ARBITRARILY LOCATED IN A THIN DIELECTRIC SLAB.....	28
VI NUMERICAL AND EXPERIMENTAL RESULTS.....	33
A. Introduction	33
B. Details of the Numerical Computations	34
VII CONCLUSIONS.....	56
REFERENCES.....	58

CHAPTER I

INTRODUCTION

A common antenna configuration is a strip conductor in or on an electrically thin dielectric slab. Such radiating systems have been in use for many years, and in 1955 an entire issue of the IRE Transactions on Microwave Theory and Techniques was devoted to microwave strip circuits.[1] The information presented was largely experimental or qualitative. Using etching techniques antennas, arrays of antennas, power dividers, impedance matching networks, and phase shifters can easily and inexpensively be fabricated on a dielectric slab. A resonant surface[2,3] can be made by etching a periodic array of dipoles, slots, or other simple elements on a dielectric slab. A simple and efficient microwave antenna can be constructed by etching a rectangular conductor on one side of a dielectric slab, while leaving the other side completely coated with metal. This configuration is termed a microstrip antenna.[4,5] Antennas printed on thin dielectric slabs can be flush mounted on aerospace vehicles, and in this way maintain the aerodynamics of the vehicle.

Despite the increasingly common use of radiating or scattering systems printed on a dielectric slab, very little theoretical analysis is available which is applicable to a wide variety of geometries. Various authors have calculated the transmission line properties of infinitely long strips on a dielectric slab.[6,7] Galejs[8] derived a stationary expression for the impedance of a strip dipole in a plane stratified medium. The design of microstrip radiators was discussed in a recent paper by Munson.[5] The purpose of this dissertation is to present a moment method solution[9] to the problem of antennas or scatterers in or on a thin dielectric slab. The analysis has the advantages that it is applicable to a wide variety of antenna geometries, and that the presence of the slab introduces no new unknown expansion modes. Unlike previous solutions, the slab may be of finite or infinite extent.

Chapter II outlines the moment method solution, based on the piecewise sinusoidal reaction formulation[10], for thin strip antennas in a homogeneous medium. In Chapter III, three methods are presented to account for the presence of an arbitrary dielectric inhomogeneity. These methods are sufficiently general to treat lossy and inhomogeneous dielectric inhomogeneities. All three methods are exact in principle, but approximate in practice. In the first of these methods, the current on the antenna and the electric field intensity in the inhomogeneity are considered to be independent unknowns. The presence of the dielectric inhomogeneity is then accounted for by increasing the size of the matrix equation which describes the wire antenna in the homogeneous medium. This method has the advantage of requiring a

minimum a priori knowledge concerning the problem, but has the disadvantage of requiring increased computer storage. In the second and third methods, the current on the wire and the electric field intensity in the inhomogeneity are treated as dependent unknowns. The presence of the inhomogeneity is accounted for by modifying the matrix equation which describes the wire antenna in the homogeneous medium. Thus, no substantial increase in computer storage is required. However, both methods require that a reasonable approximation be available to the electric field intensity radiated by a current element in the presence of the inhomogeneity.

In Chapter IV approximations are presented for the field radiated by a current expansion mode in the center of an electrically thin dielectric slab. Thus, Chapter IV yields approximations to specialize the third method presented in Chapter III to the problem of a strip antenna in the center of an electrically thin dielectric slab. The slab may be of finite or infinite extent. In Chapter V an approximate relationship is presented to relate the impedance of a strip antenna arbitrarily located in a dielectric slab to the impedance of the strip antenna in the center of a dielectric slab.

Numerical calculations, and verification by measurements and previously published results, are presented in Chapter VI for the impedance of a strip dipole in and on a thin dielectric slab. Finally, Chapter VII summarizes the results of this study and suggests methods for improving the computations.

CHAPTER II

STRIP ANTENNA IN A HOMOGENEOUS MEDIUM

The moment method solution for electrically thin circular cylindrical wire antennas in a homogeneous medium employing the sinusoidal reaction formulation is given by Richmond.[10] Paralleling Richmond's development, the moment method solution for electrically thin and perfectly conducting strip antennas in a homogeneous medium employing the sinusoidal reaction formulation will now be presented. The motivation for considering this problem is that equations derived and quantities defined will be useful when considering the effects of placing the strips in or on a thin dielectric slab, i.e., the inhomogeneous problem. If one is solely interested in thin strips in a homogeneous medium, the equivalent circular wire (referring to Fig. 2-1, $r = w/2$) can be used to give excellent pattern, current, scattering, and impedance data.[11]

Figure 2-1 shows a perfectly conducting strip antenna of width $2w$ in the homogeneous medium (μ, ϵ) . The strips are initially considered to have thickness t_0 . A local coordinate system (u, λ, v) is shown on the strip centerline. Let S denote the closed surface of the strip antenna. The external source $(\underline{J}_i, \underline{M}_i)$ generates the field $(\underline{E}, \underline{H})$ in the presence of the wire. When radiating in the homogeneous medium (μ, ϵ) without the wire, this source generates the incident field $(\underline{E}_i, \underline{H}_i)$. In this work the term wire will be used to refer to a long, slender, metallic rod which may or may not have a circular cross section. The scattered fields are defined as

$$(2-1) \quad \underline{E}_s = \underline{E} - \underline{E}_i$$

$$(2-2) \quad \underline{H}_s = \underline{H} - \underline{H}_i.$$

All sources and fields are considered to be time-harmonic, and the time dependence $e^{j\omega t}$ is suppressed.

The sources $(\underline{J}_i, \underline{M}_i)$ will induce the surface current density

$$(2-3) \quad \underline{J}_s = \hat{n} \times \underline{H}$$

on the surface S . As shown in Fig. 2-1, \hat{n} is a unit vector directed outward on S . The sources $(\underline{J}_i, \underline{M}_i)$ and \underline{J}_s generate the field $(\underline{E}, \underline{H})$ exterior to S and a null field interior to S when radiating in the presence of the wire structure. With \underline{J}_s flowing on S , we may replace the wire structure with the homogeneous medium (μ, ϵ) without disturbing the field anywhere.[12] \underline{J}_s radiates the field $(\underline{E}_s, \underline{H}_s)$ in the homogeneous medium (μ, ϵ) .

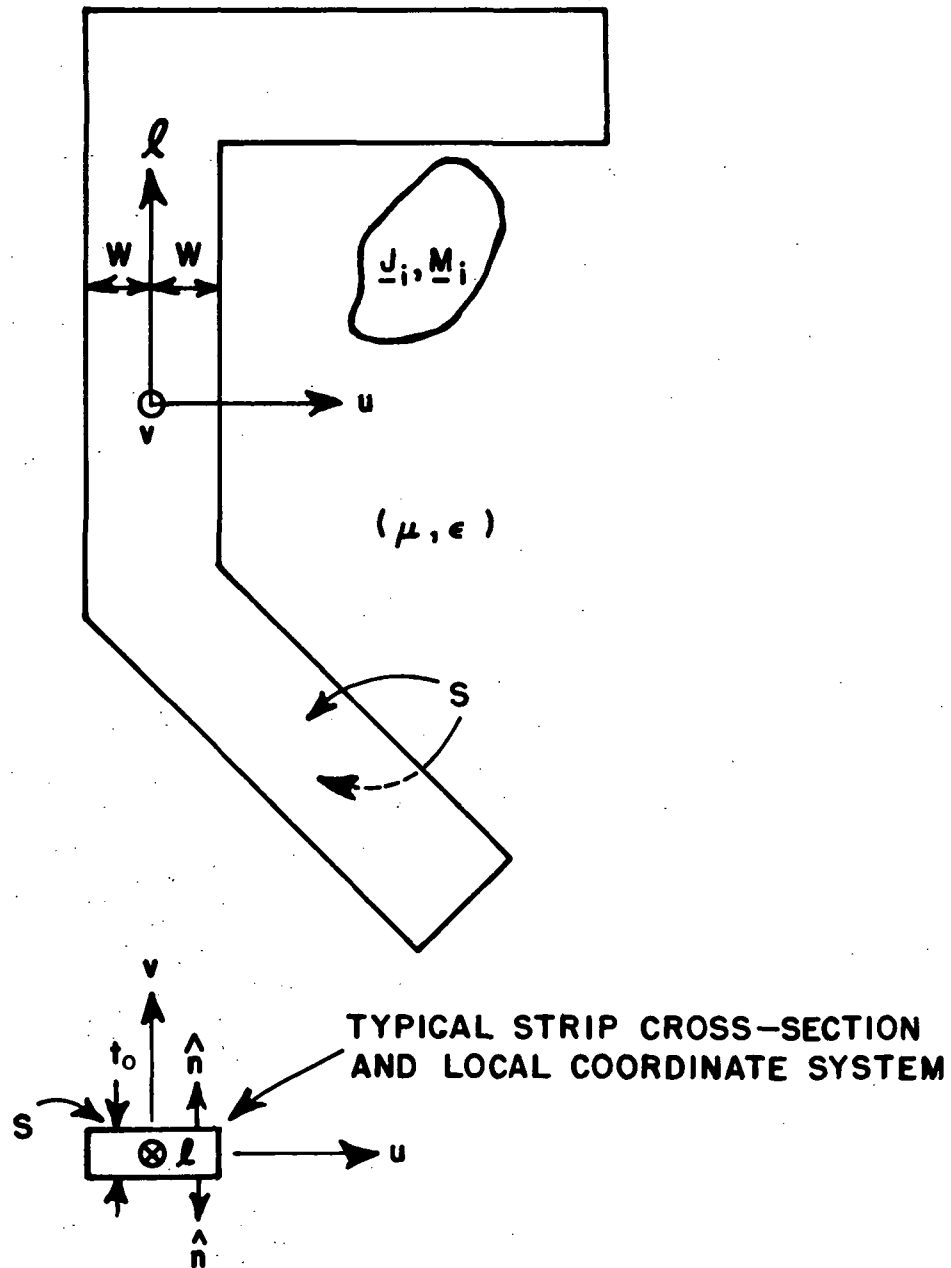


Fig. 2-1--A strip antenna in a homogeneous medium. Also shown is the strip cross-section with the local u, v coordinate system.

Consider the limiting process as the strip thickness t_0 goes to zero. In this case the scattered fields are radiated by a surface current which is the vector sum of the surface currents on the top and bottom surfaces of the strip, and will hereafter be denoted \underline{J}_S . For the strip antenna of zero thickness \underline{J}_S flows on the open surface of the strips. This open surface will hereafter be denoted S .

Now place a test source with electric surface current density \underline{J}_m and magnetic surface current density \underline{M}_m on the surface S . The reaction of the test source with the other sources is

$$(2-4) \quad \iint (\underline{J}_m \cdot \underline{E}_S - \underline{M}_m \cdot \underline{H}_S) ds = - \iint (\underline{J}_m \cdot \underline{E}_i - \underline{M}_m \cdot \underline{H}_i) ds$$

where the integration extends over the surface of the test source. Using the reciprocity theorem, Eq. (2-4) becomes

$$(2-5) \quad \iint_S \underline{J}_S \cdot \underline{E}^m ds + \iiint (\underline{J}_i \cdot \underline{E}^m - \underline{M}_i \cdot \underline{H}^m) dv = 0$$

where $(\underline{E}^m, \underline{H}^m)$ is the field of the test source radiating in the homogeneous medium, and the volume integration is over the source region. Equation (2-5) is the reaction integral equation which was developed by Rumsey[13] in 1954, and used by Richmond[10] and others.[14,15]

In general \underline{J}_S is a nonseparable function of u and ℓ . Further, \underline{J}_S is a vector function with ℓ and u components. For electrically thin wires a number of approximations can be made concerning \underline{J}_S , and these result in a simplification of the integral equation. By a thin wire it is meant that the strip width, $2w$, is much smaller than the wavelength, λ , and the wire length is much greater than the width. Other restrictions are that no wire passes within a few strip widths of another, and that no wire is bent to form a small acute angle. In this case the following approximations will be made:

1. The \hat{u} component of \underline{J}_S will be neglected.
2. \underline{J}_S is a separable function of u and ℓ .

Using the above approximations \underline{J}_S can be written as

$$(2-6) \quad \underline{J}_S = \hat{\ell} K(u) I(\ell).$$

$K(u)$ and $I(\ell)$ are functions which describe the transverse and longitudinal distribution of current along the wire, respectively. King and Harrison[16] suggest that for electrically thin and perfectly conducting strips

$$(2-7) \quad K_1(u) = \frac{c_1}{\sqrt{w^2 - u^2}}$$

where c_1 is a constant. This transverse distribution has the proper $1/\sqrt{d}$ singularity for a 360° wedge at both edges of the strip, where d denotes the distance from the edge [17]. A second transverse distribution which also has the proper edge behavior is

$$(2-8) \quad K_2(u) = \frac{c_2}{\sqrt{\rho}} + \frac{c_2}{\sqrt{\rho'}}$$

where c_2 is a constant and

$$\left. \begin{array}{l} (2-9a) \quad \rho = w - u \\ (2-9b) \quad \rho' = w + u \end{array} \right\} |u| \leq w.$$

The constants c_1 and c_2 can be evaluated by requiring

$$(2-10) \quad \int_{-w}^w K(u) du = 1.$$

Substituting Eqs. (2-7) and (2-8) into Eq. (2-10) yields $c_1 = 1/\pi$ and $c_2 = 1/4\sqrt{2w}$. For strip antennas in a homogeneous medium, this author knows of no reason to prefer either of the distributions of Eqs. (2-7) and (2-8), or any of a variety of additional possibilities, and we choose to use $K_1(u)$. Inserting Eq. (2-7) into Eq. (2-6) yields

$$(2-11) \quad \underline{J}_s = \frac{\hat{e}_l I(l)}{\pi \sqrt{w^2 - u^2}}.$$

Using Eq. (2-11), Eq. (2-5) simplifies to

$$(2-12) \quad \frac{-1}{\pi} \int_0^L \int_{-w}^w \frac{I(l)}{\sqrt{w^2 - u^2}} E_l^m du dl = V_m$$

where L denotes the overall wire length and

$$(2-13a) \quad V_m = \iiint (\underline{J}_i \cdot \underline{E}^m - \underline{M}_i \cdot \underline{H}^m) dv$$

$$(2-13b) \quad \underline{E}_\ell^m = \underline{E}_m \cdot \hat{\ell}.$$

In Eq. (2-13a) the integration is over the source region.

Equation (2-12) is the thin strip integral equation to be solved for $I(\ell)$. In this equation \underline{E}_ℓ^m and V_m are considered to be known. To solve for the current, suitable test sources and expansion modes will now be defined.

The test source is chosen as a filamentary electric dipole line source with a sinusoidal current distribution. This choice has three advantages:

1. The near zone fields are available in terms of simple closed form expressions.[18]

2. The mutual impedance between two sinusoidal dipoles is available in terms of exponential integrals.[18]

3. The piecewise-sinusoidal function closely approximates the natural current distribution on a perfectly conducting thin wire.

A typical test source is shown in Fig. 2-2. It is a filamentary V dipole consisting of two segments which in general have unequal lengths and may intersect at any angle. The V dipole of Fig. 2-2 is shown intersecting at an angle of 180° for simplicity. Note that the dipole current is zero at the endpoints, rises sinusoidally to a maximum at the terminals, and has a slope discontinuity at the terminals. The functional form for the test source current distribution is

$$(2-14) \quad \underline{F}_t(\ell) = \left[\frac{\hat{\ell}_1 P_1 \sinh \gamma(\ell - \ell_1)}{\sinh \gamma d_1} + \frac{\hat{\ell}_2 P_2 \sinh \gamma(\ell_3 - \ell)}{\sinh \gamma d_2} \right]$$

where $\hat{\ell}_1$ is a unit vector pointing from ℓ_1 to ℓ_2 , $\hat{\ell}_2$ is a unit vector pointing from ℓ_2 to ℓ_3 , d_1 and d_2 are the lengths of the segments from ℓ_1 to ℓ_2 and ℓ_2 to ℓ_3 respectively, and

$$(2-15a) \quad P_1 = \begin{cases} 1 & \ell_1 \leq \ell \leq \ell_2 \\ 0 & \text{otherwise} \end{cases}$$

$$(2-15b) \quad P_2 = \begin{cases} 1 & \ell_2 \leq \ell \leq \ell_3 \\ 0 & \text{otherwise} \end{cases}$$

$$(2-15c) \quad \gamma = j\omega\sqrt{\mu\epsilon} \quad .$$

The test dipole has unit terminal current and is located on the ℓ axis. For $F_t(\ell)$ to have the advantages listed above, γ must be given by Eq. (2-15c).

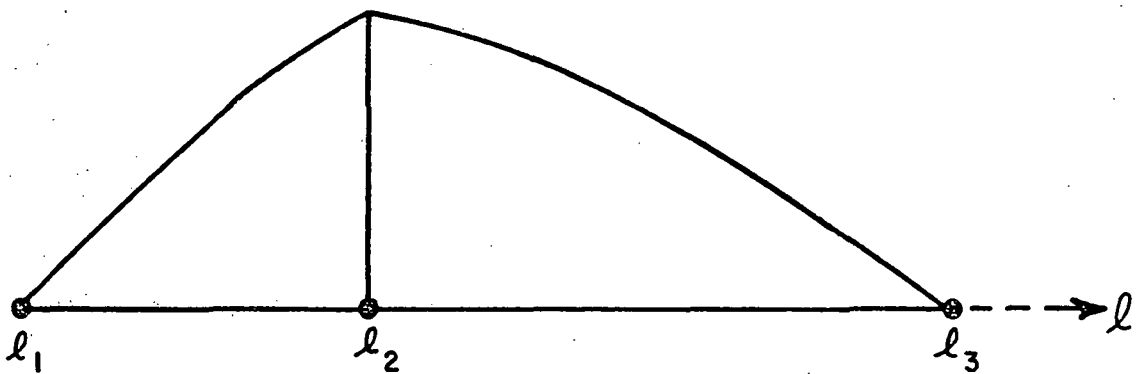


Fig. 2-2--A linear test dipole and its sinusoidal current distribution. The endpoints are at ℓ_1 and ℓ_3 with terminals at ℓ_2 .

For a typical problem Eq. (2-12) would be enforced for N test dipoles located at different positions along the wire axis. In this case, Eq. (2-12) represents a system of N simultaneous integral equations with $m = 1, 2, \dots, N$. We will use the notation that F_{tm} is the m th test dipole which radiates the field $(\underline{E}^m, \underline{H}^m)$ in the homogeneous medium (μ, ϵ) . To obtain a system of N simultaneous linear equations the surface current density, \underline{J}_s , will be expanded in terms of a set of basis functions as follows:

$$(2-16) \quad \underline{J}_s(u, \ell) = \sum_{n=1}^N I_n \underline{F}_{en}^C(u, \ell) \quad .$$

The expansion modes are electric dipole surface currents which are simply related to the filamentary test dipoles by

$$(2-17) \quad \underline{F}_{en}^C(u, \ell) = K_1(u) \underline{F}_{tn}(u, \ell) = \frac{1}{\pi \sqrt{w^2 - u^2}} \underline{F}_{tn}(\ell).$$

The superscript c on \underline{F}_{en}^C emphasizes that it is a conduction current. Note that \underline{F}_{en}^C has unit terminal current and that the nth filamentary test dipole is located on the center line of the nth surface current expansion mode. Using Eqs. (2-11), (2-16) and (2-17)

$$(2-18) \quad I(\ell) = \sum_{n=1}^N I_n \underline{F}_{tn}(\ell).$$

Inserting Eq. (2-18) into Eq. (2-12) yields the following system of simultaneous linear equations:

$$(2-19) \quad \sum_{n=1}^N I_n Z_{mn} = V_m \quad m = 1, 2, \dots, N$$

where the elements of the open-circuit impedance matrix are

$$(2-20) \quad Z_{mn} = \frac{-1}{\pi} \iint_n \frac{1}{\sqrt{w^2 - u^2}} \underline{F}_{tn}(\ell) \underline{E}_{\ell}^m du d\ell.$$

In Eq. (2-20) the integration extends over the surface of the two segments making up the nth expansion mode. Equation (2-19) can be written as the matrix equation

$$(2-21) \quad ZI = V$$

where Z denotes the N by N impedance matrix, I is the current column, and V is the voltage column.

If the equivalent radius concept is used then Eq. (2-20) is replaced by [10]

$$(2-22) \quad Z_{mn} = - \iint_n \underline{F}_{tn}(\ell) \cdot \underline{E}^m(\ell, \phi) d\ell d\phi$$

where the integration is over the circular cylindrical surface $\rho = w/2$ in the range of the nth expansion mode \underline{F}_n . The expansion mode \underline{F}_n is a surface current given by

$$(2-23) \quad \underline{F}_n(\ell) = \frac{1}{2\pi a} \underline{F}_{tn}(\ell)$$

10

where $a = w/2$. $\underline{F}_n(\ell)$ exists on the surface $\rho = a$. Computer programs are available to evaluate Eq. (2-22) and Eq. (2-13a) if the source is a delta-gap generator or a plane wave.[14]

Z_{mn} is the mutual impedance between the m th test filamentary dipole and the n th surface expansion dipole. Since the test and expansion modes are not identical, the reciprocity theorem can not be used to demonstrate the symmetry of the impedance matrix. However, in practice the matrix will be considered symmetric.[10] The symmetric matrix requires that $(N^2+N)/2$ elements be evaluated and stored, as compared to N^2 for the full matrix. As has been mentioned, the longitudinal integration of Eq. (2-20) is available in closed form, and computer subroutines are also available[18,19]. This author knows of no closed form expression for the transverse integration of Eq. (2-20), and thus, if the equivalent radius concept is not being used, numerical integration is employed. For segments with one or two points in common the transverse integration has an integrable logarithmic singularity at $u = 0$. A $1/\sqrt{u}$ singularity at $u = \pm w$ is present for all evaluations of Eq. (2-20). Numerically these singularities can be handled by using closely spaced points and integration formulas which avoid $u = 0$ or $\pm w$.

The effects of lumped loading may be easily accounted for in precisely the same fashion as is used for circular-cylindrical wires[10]. Briefly, Eq. (2-19) is replaced by

$$(2-24) \quad \sum_{n=1}^N \bar{Z}_{mn} I_n = V_m$$

where \bar{Z}_{mn} is obtained from Z_{mn} by simply modifying the diagonal elements as follows

$$(2-25) \quad \bar{Z}_{mm} = Z_{mm} + Z_m$$

and Z_m denotes the impedance of the lumped load.

In general the excitation voltages of Eqs. (2-19) or (2-24) must be evaluated using Eq. (2-13a). For the simple delta-gap model of a voltage generator, Eq. (2-13a) reduces to

$$(2-26) \quad V_m = v_m$$

where v_m is the complex magnitude of the voltage generator inserted at the terminals of the m th expansion mode. According to this model V_m is non-zero only if a generator is at the terminals of the m th expansion mode.

CHAPTER III

STRIP ANTENNA IN THE PRESENCE OF AN ARBITRARY DIELECTRIC INHOMOGENEITY

A. Introduction

In this chapter the equations of the previous chapter are modified to account for a dielectric inhomogeneity. Figure 3-1 shows a perfectly conducting strip antenna in the presence of a dielectric inhomogeneity confined to the volume V . The parameters of the ambient medium are (μ, ϵ) , and the volume V contains a dielectric with parameters (μ, ϵ_2) . The parameters ϵ and ϵ_2 may be complex, and ϵ_2 may be a function of position. We now have a known current distribution $(\underline{J}_i, \underline{M}_i)$ radiating in the presence of two inhomogeneities, the wire and the dielectric inhomogeneity. $(\underline{E}, \underline{H})$ denotes the fields radiated by $(\underline{J}_i, \underline{M}_i)$ in the presence of the two inhomogeneities. We wish to replace the inhomogeneities by equivalent currents. As described in Chapter II the perfectly conducting strips can be replaced by the surface currents \underline{J}_s . Using Rhodes' [20] volume equivalence theorem the dielectric inhomogeneity may be replaced with the ambient medium and the equivalent volume electric current density

$$(3-1) \quad \underline{J} = j\omega(\epsilon_2 - \epsilon)\underline{E}$$

where \underline{E} is the electric field intensity in the dielectric inhomogeneity. \underline{J} exists only in V , and is in general unknown since \underline{E} is unknown. The currents $(\underline{J}_i, \underline{M}_i)$, \underline{J}_s , and \underline{J} radiate the fields $(\underline{E}, \underline{H})$ in the homogeneous medium (μ, ϵ) .

The reaction integral equation, Eq. (2-5), and Eq. (2-13a) are modified by replacing \underline{J}_i by $\underline{J}_i + \underline{J}$. Thus, \underline{J} is considered as a source term, similar to \underline{J}_i . If \underline{E} is known or if a sufficiently accurate approximation for \underline{E} is available, the results of the preceding section can be used directly by replacing \underline{J}_i with $\underline{J}_i + \underline{J}$. Unfortunately, a good approximation to \underline{E} is generally not available. In this case at least two approaches to the problem can be used. The first is to consider the current on the wire and the electric field intensity in the inhomogeneity to be independent unknowns, and the second is to consider the wire current and \underline{E} to be dependent unknowns. The remainder of the chapter will describe these two approaches. Two different methods will be presented for treating the wire current and \underline{E} as dependent unknowns.

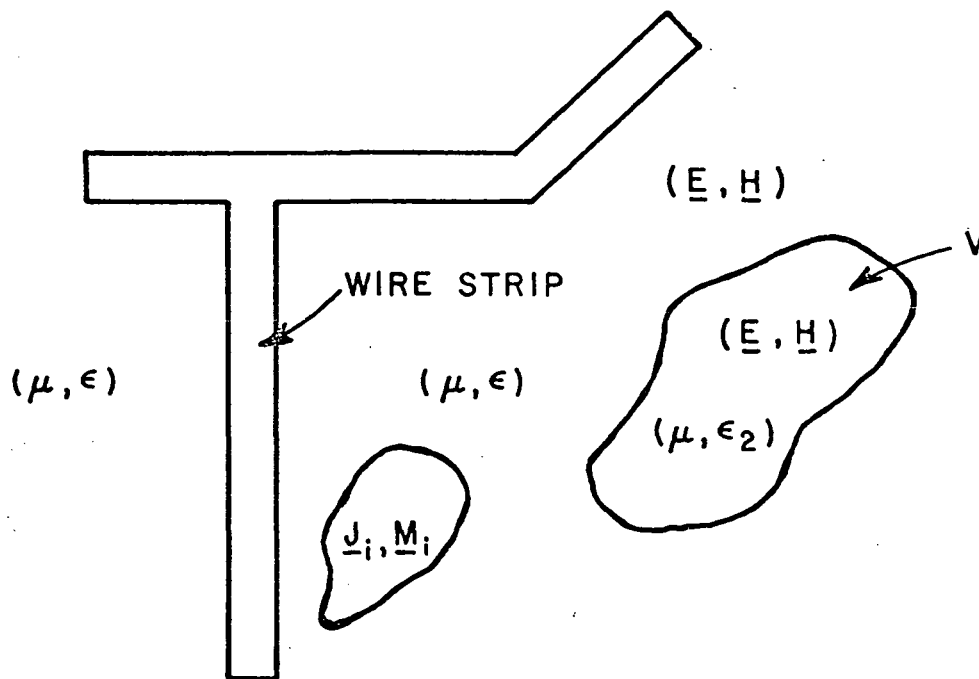


Fig. 3-1--A strip antenna in the presence of a dielectric inhomogeneity.

B. Approach 1 - The Wire Current and the Electric Field in the Inhomogeneity are Considered to be Independent Unknowns

In this section it will be shown how the matrix equation (2-21) is altered if the electric field intensity in the inhomogeneity, \underline{E} , and the wire current are treated as independent unknowns. As a first step, the equivalent volume polarization currents defined by Eq. (3-1) are expanded in terms of a set of M basis functions as follows:

$$(3-2) \quad \underline{J} = \sum_{n=N+1}^{N+M} I_n \underline{G}_n.$$

Comparing Eqs. (2-16) and (3-2) the current on the wire is expanded in terms of the N unknowns I_n ($n = 1, 2 \dots N$), and the volume polarization currents are expanded in terms of the M unknowns I_n ($n = N+1, N+2, \dots N+M$).

As was mentioned above, Eq. (2-5) is modified by replacing \underline{J}_i with $\underline{J}_i + \underline{J}$ and becomes

$$(3-3) \quad \iint_S \underline{J}_s \cdot \underline{E}^m ds + \iiint [(\underline{J}_i + \underline{J}) \cdot \underline{E}^m - \underline{M}_i \cdot \underline{H}^m] dv = 0$$

where the volume integration extends through the source region and V . Equation (3-3) mathematically expresses the fact that there is zero reaction between the m th test source located on the wire axis and the sum of the currents \underline{J}_S , \underline{J} , \underline{J}_i , and \underline{M}_i . Rearranging Eq. (3-3) so that only unknown currents appear on the left hand side of the equation yields

$$(3-4) \quad \iint_S \underline{J}_S \cdot \underline{E}^m ds - \iiint_V \underline{J} \cdot \underline{E}^m dv = V_m$$

where V_m is given by Eq. (2-13a).

Enforcing Eq. (3-4) for N test sources, described by Eq. (2-14), yields the following system of simultaneous linear equations:

$$(3-5) \quad \sum_{n=1}^{N+M} I_n Z_{mn} = V_m \quad m = 1, 2 \dots N.$$

In Eq. (3-5) the Z_{mn} are given by Eq. (2-20) for $m \leq N$ and by

$$(3-6) \quad Z_{mn} = - \iiint_V \underline{G}_n \cdot \underline{E}^m dV$$

for $n > N$ (and $m \leq N$).

Equation (3-5) represents N linearly independent equations in $N+M$ unknowns. In order to solve for the I_n we must obtain an additional M linearly independent equation.

The additional M equations will be obtained by using the fact that the sum of the electric field intensities radiated by \underline{J}_S , \underline{J} , \underline{J}_i , and \underline{M}_i in the presence of the homogeneous medium (μ, ϵ) is \underline{E} in V , the volume occupied by the dielectric inhomogeneity. Denoting \underline{E}_S , \underline{E}_V , and \underline{E}_i as the electric field intensities radiated by the sources \underline{J}_S , \underline{J} , and $(\underline{J}_i, \underline{M}_i)$ respectively in the homogeneous medium (μ, ϵ) we then have

$$(3-7) \quad \underline{E}_S + \underline{E}_V + \underline{E}_i = \underline{E} \text{ in } V.$$

Now define a series of M vector weighting functions \underline{H}_m ($m = N+1, N+2, \dots N+M$), and integrating over the volume V yields

$$(3-8) \quad \iiint_V (\underline{E}_s + \underline{E}_v - \underline{E}) \cdot \underline{H}_m \, dv = - \iiint_V \underline{E}_i \cdot \underline{H}_m \, dv$$

$$m = N+1, N+2, \dots, N+M.$$

If we denote \underline{E}_{sn} as the electric field intensity radiated by \underline{F}_{en}^C (see Eq. (2-16)) and \underline{E}_{vn} as the electric field intensity radiated by \underline{G}_n (see Eq. (3-2)) then using Eqs. (2-16), (3-1), and (3-2) in Eq. (3-8) yields

$$(3-9) \quad \sum_{n=1}^N I_n \iiint_V \underline{E}_{sn} \cdot \underline{H}_m \, dv + \sum_{n=N+1}^{N+M} I_n \iiint_V \left[\underline{E}_{vn} - \frac{\underline{G}_n}{j\omega(\epsilon_2 - \epsilon)} \right] \cdot \underline{H}_m \, dv$$

$$= - \iiint_V \underline{E}_i \cdot \underline{H}_m \, dv \quad m = N+1, N+2, \dots, N+M.$$

Equation (3-9) represents the additional M equations in the $N+M$ unknowns I_n ($n = 1, 2, \dots, N+M$). Equation (3-9) can be written as

$$(3-10) \quad \sum_{n=1}^{N+M} I_n Z_{mn} = V_m \quad m = N+1, N+2, \dots, N+M$$

where

$$(3-11) \quad Z_{mn} = \iiint_V \underline{E}_{sn} \cdot \underline{H}_m \, dv \quad n = 1, 2, \dots, N$$

$$(3-12) \quad Z_{mn} = \iiint_V \left[\underline{E}_{vn} - \frac{\underline{G}_n}{j\omega(\epsilon_2 - \epsilon)} \right] \cdot \underline{H}_m \, dv$$

$$n = N+1, N+2, \dots, N+M$$

$$(3-13) \quad V_m = - \iiint_V \underline{E}_i \cdot \underline{H}_m \, dv \quad n = 1, 2, \dots, N+M.$$

Equation (3-5) together with Eq. (3-10) represent $N+M$ equations in the $N+M$ unknowns I_n ($n = 1, 2, \dots, N+M$). Equations (3-5) and (3-10) can be expressed in matrix form as

$$(3-14) \quad ZI = V$$

where Z denotes a square matrix, I is an unknown column vector, and V is a known column vector. The elements of Z , denoted Z_{mn} , and the elements of V , denoted V_m , are given by different expressions depending on the values of m and n . The matrix Eq. (3-14) is symbolically shown in Fig. 3-2 where the matrix is divided into four regions and the column vectors into two regions. In Table 1 these regions are defined and the equations to use for Z_{mn} and V_m are listed.

TABLE 1

Region	Definition of Region	Z_{mn} or V_m Given By
Z_A	$1 \leq m \leq N, \quad 1 \leq n \leq N$	Eq. (2-20) or (2-22)
Z_B	$1 \leq m \leq N, \quad N+1 \leq n \leq N+M$	Eq. (3-6)
Z_C	$N+1 \leq m \leq N+M, \quad 1 \leq n \leq N$	Eq. (3-11)
Z_D	$N+1 \leq m \leq N+M, \quad N+1 \leq n \leq N+M$	Eq. (3-12)
V_{AB}	$1 \leq m \leq N$	Eq. (2-13a)
V_{CD}	$N+1 \leq m \leq N+M$	Eq. (3-13)

The above approach has the advantage that no a priori knowledge of the fields is required, and the solution can approach the exact solution for a sufficiently large number of basis functions. Mutual interactions among various portions of the dielectric body and the wire as well as surface-wave excitation are automatically included. Further, if J is expanded in subsectional basis functions, the method is not restricted by the shape of the dielectric body (i.e., by the shape of the volume V). The main restriction is that the dimensions of the inhomogeneity not be large in terms of the wavelength. For example in a dielectric slab one wavelength square and less than $1/20$ wavelength thick, one might divide the slab into 100 cells. If each cell is considered to have three unknown field components, there are a total of 300 unknowns representing the slab. Assuming a symmetric impedance matrix, 45, 150 impedance elements would have to be evaluated and stored for region Z_D alone. Thus, while this method does have considerable advantage for electrically small inhomogeneities and some two dimensional problems[21,22], it is limited by the speed and storage capabilities of the digital computer being used.

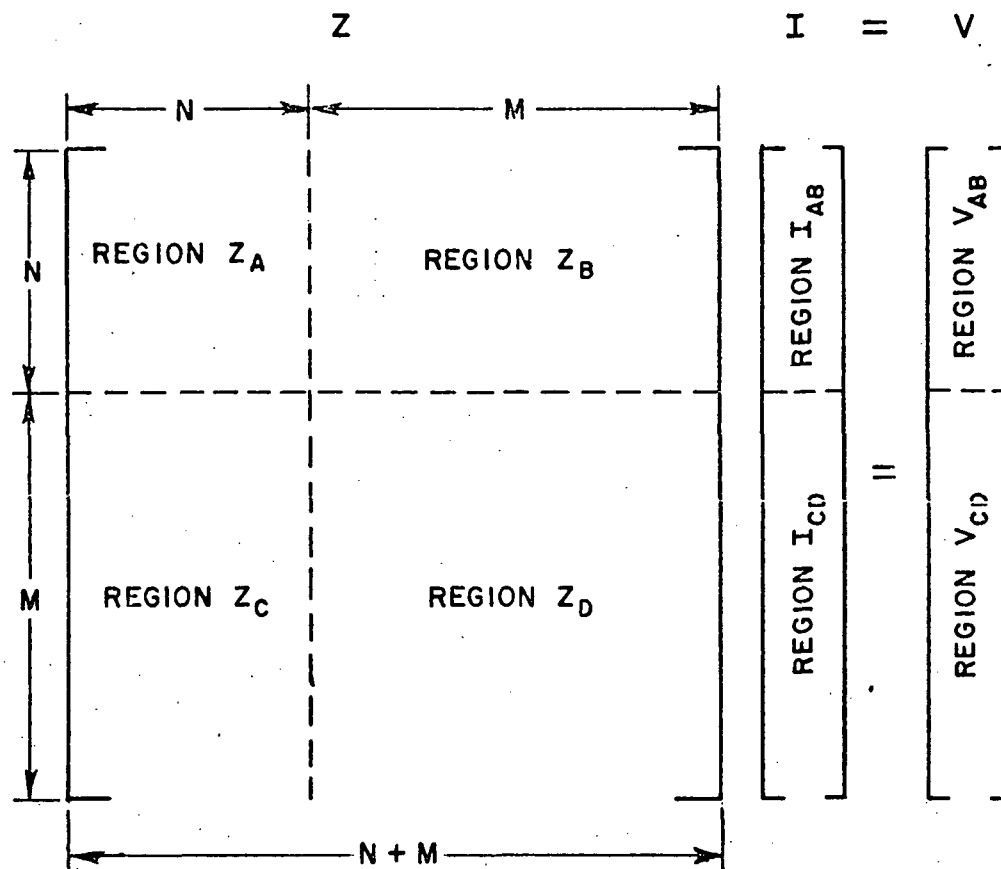


Fig. 3-2. Symbolic representation of the matrix equation $ZI = V$.

C. Approach 2 - The Wire Current and the Electric Field in the Inhomogeneity are Considered to be Dependent Unknowns

In this section two formulations will be presented for treating a wire antenna in the presence of a dielectric inhomogeneity, and where the current on the wire and the fields in the inhomogeneity are treated as dependent unknowns. Both approaches will account for the inhomogeneity by modifying the impedance matrix which describes the wire antenna in the homogeneous medium.

Equation (2-5) is an integral equation for the current \underline{J}_S on a perfectly conducting wire structure which is immersed in the homogeneous medium (μ, ϵ) and excited by the sources $(\underline{J}_i, \underline{M}_i)$. Here $(\underline{E}^m, \underline{H}^m)$ denotes the fields of the test source radiating in the homogeneous medium (μ, ϵ) . If in Eq. (2-5) $(\underline{E}^m, \underline{H}^m)$ is taken to be the fields of the test source radiating in an inhomogeneous medium, then Eq. (2-5) becomes an integral equation for \underline{J}_S on the perfectly

conducting wire in the inhomogeneous medium, and excited by the sources $(\underline{J}_i, \underline{M}_i)$. Here the inhomogeneity is the dielectric volume and not the wire. As before, with $(\underline{E}^m, \underline{H}^m)$ defined in this way, Eq. (2-5) insures that there will be zero reaction between the test source located on the strip axis and \underline{J}_S and $(\underline{J}_i, \underline{M}_i)$. Clearly Eqs. (2-13a) and (2-20) yield the elements of the voltage column and the impedance matrix for the wire in the inhomogeneous medium with the new definition of $(\underline{E}^m, \underline{H}^m)$.

The fields of the mth test source in the inhomogeneous medium can be expressed as

$$(3-15) \quad \underline{E}^m = \underline{E}_O^m + \underline{E}_D^m$$

$$(3-16) \quad \underline{H}^m = \underline{H}_O^m + \underline{H}_D^m$$

where $(\underline{E}_O^m, \underline{H}_O^m)$ are the fields of the mth test source radiating in the homogeneous medium (μ, ϵ) , and $(\underline{E}_D^m, \underline{H}_D^m)$ is the perturbation in the fields caused by the inhomogeneity. Substituting Eqs. (3-15) and (3-16) into Eqs. (2-13a) and (2-20) yields

$$(3-17) \quad V_m = \iiint [\underline{J}_i \cdot (\underline{E}_O^m + \underline{E}_D^m) - \underline{M}_i \cdot (\underline{H}_O^m + \underline{H}_D^m)] dv$$

$$(3-18) \quad Z_{mn} = -\frac{1}{\pi} \iint_n \frac{1}{\sqrt{w^2 - u^2}} \underline{F}_{tn}(l) \cdot (\underline{E}_O^m + \underline{E}_D^m) du dl.$$

Thus, in the presence of the dielectric inhomogeneity, the matrix Eq. (2-21) becomes

$$(3-19) \quad (Z + \Delta Z) I = (V + \Delta V)$$

where the elements of Z and V are given by Eqs. (2-20) and (2-13a) respectively, and the elements of ΔZ and ΔV are given by

$$(3-20) \quad \Delta Z_{mn} = -\frac{1}{\pi} \iint_n \frac{1}{\sqrt{w^2 - u^2}} \underline{F}_{tn}(l) \cdot \underline{E}_D^m du dl$$

$$(3-21) \quad \Delta V_m = \iiint \underline{J}_i \cdot \underline{E}_D^m - \underline{M}_i \cdot \underline{H}_D^m dv.$$

If the equivalent round wire for the strip is used, then the elements of Z are given by Eq. (2-22), and the elements of ΔZ are given by

$$(3-22) \quad \Delta Z_{mn} = - \iint_n \underline{F}_n(\ell) \cdot \underline{E}_D^m(\ell, \phi) d\ell d\phi.$$

Clearly this approach is useful only if the fields of the test source in the presence of the inhomogeneity, or a good approximation to these fields, is known. One important example where this is the case is an antenna in the vicinity of a dielectric half-space. For this inhomogeneity exact expressions as well as many useful approximations are available for the fields of infinitesimal current sources in the vicinity of the dielectric half-space[23-26]. Further, a solution similar to that presented above has been used to find the current distribution, impedance, and field patterns of antennas in the presence of a dielectric half-space.[27]

Next a different formulation will be presented for including the effects of the dielectric inhomogeneity, and where the current on the wire and the fields in the dielectric inhomogeneity are considered to be dependent unknowns. This will be done by modifying the expansion functions on the wire, and again will result in a modification to the impedance matrix. All of the numerical calculations to be presented in Chapter VI are based on this method.

Figure 3-3 shows the n th expansion mode radiating in the presence of the dielectric inhomogeneity. The field radiated by \underline{F}_{en}^C is denoted by $(\underline{E}_{en}^C, \underline{H}_{en}^C)$, and what follows assumes that a good approximation to \underline{E}_{en}^C is available. The equations to follow shed no light on the generally difficult problem of determining \underline{E}_{en}^C , but rather show how a knowledge of \underline{E}_{en}^C can be used to find the current on the wire.

In the absence of the dielectric inhomogeneity the expansion modes were the conduction currents \underline{F}_{en}^C defined in Eq. (2-17). In the presence of the dielectric inhomogeneity the expansion modes will be

$$(3-23) \quad \underline{F}_{en} = \underline{F}_{en}^C + \underline{F}_{en}^P$$

where

$$(3-24) \quad \underline{F}_{en}^P = j\omega(\epsilon_2 - \epsilon) \underline{E}_{en}^C.$$

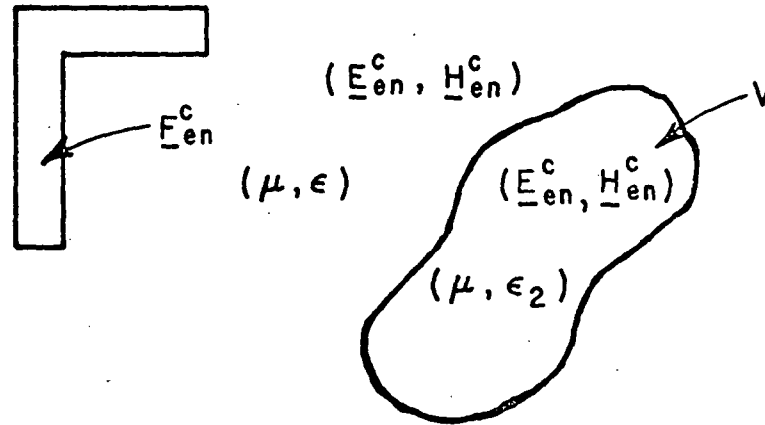


Fig. 3-3--The nth expansion mode radiating in the presence of a dielectric inhomogeneity.

The fields of the expansion modes defined by Eqs. (3-23) and (3-24) each satisfy boundary conditions at the dielectric interface. Thus, any linear combination of these modes will also satisfy boundary conditions at the dielectric interface. The volume polarization current \underline{F}_{en}^p exists only in the volume V . In the presence of a dielectric inhomogeneity the expansion modes are made up of two distinct parts. The first part is a conduction current given by Eq. (2-17). The second is a volume polarization current confined to the volume V and given by Eq. (3-24). The mutual impedance matrix is modified by adding to each element

$$(3-25) \quad \Delta Z_{mn} = - \iiint_V \underline{F}_{en}^p \cdot \underline{E}_m^c dv.$$

The current on the wire in the presence of the dielectric inhomogeneity is given by the solution of the following set of linear simultaneous equations

$$(3-26) \quad \sum_{n=1}^N I_n (Z_{mn} + \Delta Z_{mn}) = V_m \quad \text{where } m = 1, 2, \dots, N.$$

Equation (3-26) can be written in matrix form as

$$(3-27) \quad (Z + \Delta Z) I = V$$

where $Z + \Delta Z$ is an N by N impedance matrix, I is the current column, and V is the voltage column. The elements of Z are given by Eqs. (2-20) or (2-22), and the elements of V are given by Eq. (2-13a). The elements of ΔZ are given by Eq. (3-25). Comparing Eqs. (2-21) and (3-27) or Eqs. (2-19) and (3-26) it is seen that the presence of the dielectric inhomogeneity introduces no new unknowns, and thus the size of the impedance matrix is unchanged. The presence of the inhomogeneity is accounted for entirely by a modification of the elements in the square impedance matrix.

It is interesting that Eq. (3-25) vanishes for two special cases. First, as the volume of the inhomogeneity V approaches zero, ΔZ_{mn} must also go to zero. Second, as ϵ_2 approaches ϵ , F_{en}^D goes to zero, and thus so must ΔZ_{mn} . Thus, this formulation automatically reduces to the correct limit as the volume of the inhomogeneity approaches zero, or as ϵ_2 approaches ϵ .

The obvious advantage of treating the electric field in the inhomogeneity as a dependent rather than an independent unknown is that no new unknowns are introduced, and the size of the impedance matrix is not increased. If $(\underline{E}_D^m, \underline{H}_D^m)$ or \underline{E}_{en}^C are known exactly, then using the above equations, the presence of the inhomogeneity can be treated exactly. Unfortunately, even good approximations to $(\underline{E}_D^m, \underline{H}_D^m)$ or \underline{E}_{en}^C are often not available. In treating antennas in the presence of dielectric inhomogeneities by the last two methods, the real problem is to determine suitable approximations for either $(\underline{E}_D^m, \underline{H}_D^m)$ or \underline{E}_{en}^C . The next chapter considers the problem of determining \underline{E}_{en}^C for a strip antenna in the center of an electrically thin dielectric slab.

CHAPTER IV STRIP ANTENNA LOCATED IN THE CENTER OF A THIN DIELECTRIC SLAB

In the preceding chapter equations were presented to analyze an electrically thin strip antenna radiating in the presence of an arbitrarily shaped dielectric inhomogeneity. Referring to Fig. 3-3, these equations were developed with the understanding that for the particular inhomogeneity of interest a good approximation to \underline{E}_{en}^C was available. The purpose of this section is to present approximations for \underline{E}_{en}^C for the case of an electrically thin strip antenna located in the center of an electrically thin dielectric slab.

A typical configuration is shown in Fig. 4-1. The strip antenna is in the center of a slab of dimensions L_1 by L_2 by T . The strips are in a plane a distance $T/2$ from either of the broad surfaces of the slab. T is considered to be much less than a wavelength in either the ambient medium (μ, ϵ) or the slab medium (μ, ϵ_2) . \underline{E}_{en}^C is defined as the electric field intensity of the n th sinusoidal electric surface current dipole expansion mode, \underline{F}_{en}^C of Eq. (2-17) in the presence of the slab. We will be concerned with determining expressions for \underline{E}_{en}^C for field points in the dielectric slab.

Figure 4-2 shows one segment of \underline{F}_{en}^C . Also shown is the near-zone region A defined by

$$\left. \begin{aligned} -U_{\max} &\leq u \leq U_{\max} \\ \ell_1 &\leq \ell \leq \ell_2 \\ -T/2 &\leq v \leq T/2 \end{aligned} \right\} \text{ region A.}$$

Region B is the entire slab except for region A.

The surface current on the segment can be written as (see Eqs. (2-1), (2-15), and (2-17))

$$\begin{aligned} (4-1) \quad \underline{J}_s(u, \ell) &= \hat{x} K_1(u) \left[\frac{I_1 \sinh \gamma(\ell_2 - \ell) + I_2 \sinh \gamma(\ell - \ell_1)}{\sinh \gamma d} \right] \\ &= \hat{x} K_1(u) f(I_1, I_2, \ell) \end{aligned}$$

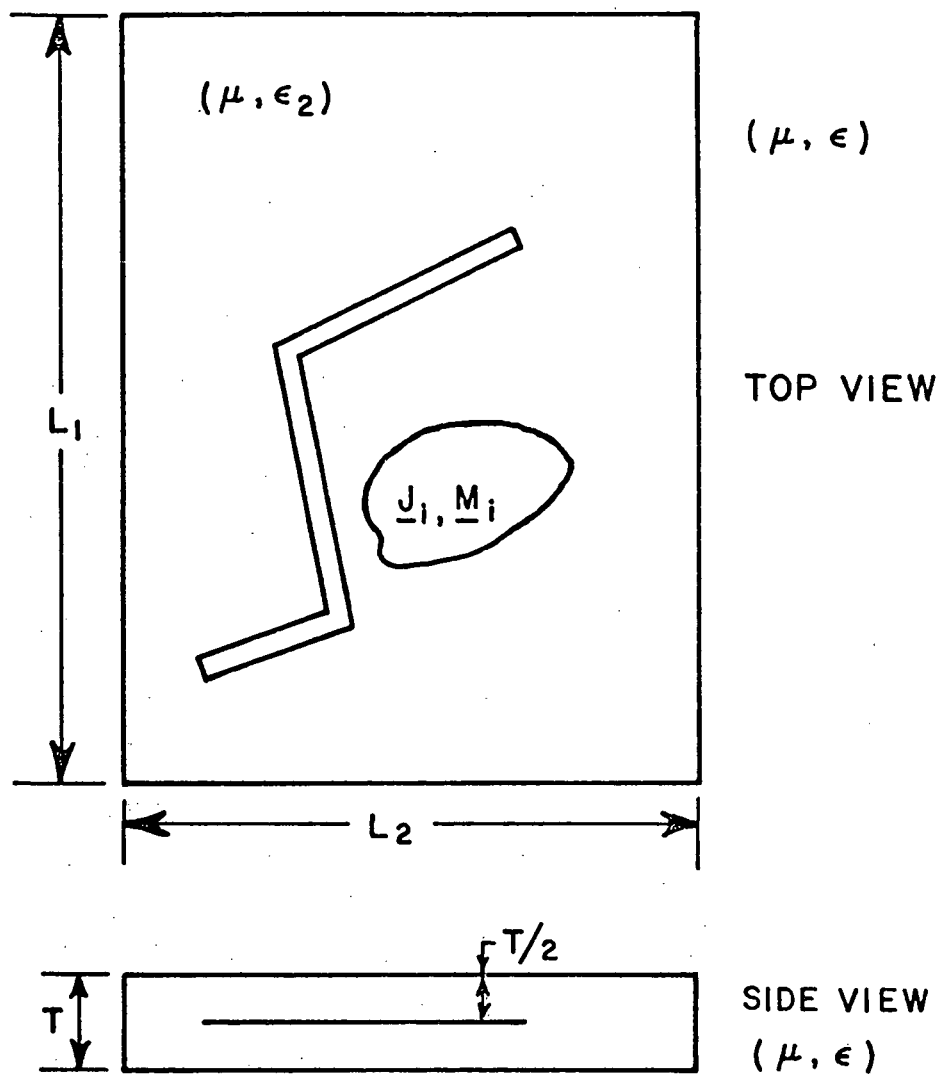


Fig. 4-1--A strip antenna in the center of a thin dielectric slab.

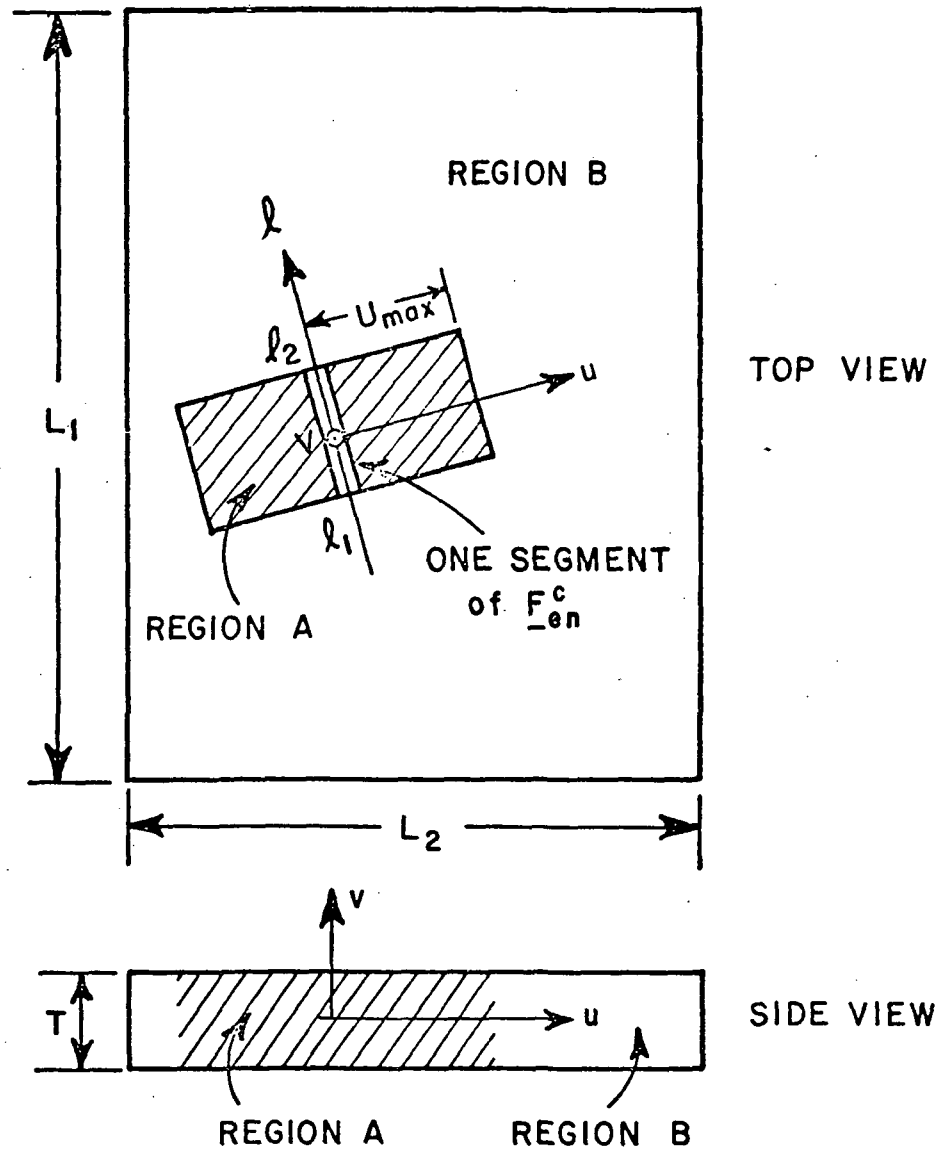


Fig. 4-2--Definition of regions A and B.

where I_1 or I_2 , but not both, are unity. The equation of continuity is

$$(4-2) \quad \nabla \cdot \underline{J}_S = -j\omega\rho_S$$

where ρ_S is the surface charge density. Solving Eq. (4-2) for ρ_S and using Eq. (4-1) yields

$$(4-3) \quad \rho_S(u, \ell) = - \frac{\nabla \cdot \underline{J}_S}{j\omega} = - \frac{K_1(u)}{j\omega} f'(I_1, I_2, \ell)$$

where the prime implies differentiation with respect to ℓ .

We will denote $\underline{D}_{\text{above}}$ and $\underline{D}_{\text{below}}$ as the electric flux density at the upper and lower surfaces of the strip, respectively. From boundary conditions at the surface of the strip

$$(4-4) \quad \hat{v} \cdot \underline{D}_{\text{above}} + (-\hat{v}) \cdot \underline{D}_{\text{below}} = \rho_S(u, \ell).$$

Since the strip is considered to be in the center of the slab we have from symmetry $\underline{D}_{\text{above}} = -\underline{D}_{\text{below}}$, and Eq. (4-4) becomes

$$(4-5) \quad \underline{D}_{\text{above}} = \hat{v} \rho_S(u, \ell)/2$$

and

$$(4-6) \quad \underline{E}_{\text{above}} = \hat{v} \rho_S(u, \ell)/2\epsilon_2.$$

Using Eq. (4-3), Eq. (4-6) becomes

$$(4-7) \quad \underline{E}_{\text{above}} = \frac{-\hat{v} K_1(u)}{2j\omega \epsilon_2} f'(I_1, I_2, \ell).$$

Eq. (4-7) predicts that $\underline{E}_{\text{above}}$ is a function of the permittivity of the slab, but not its dimensions. In fact Eq. (4-7) yields $\underline{E}_{\text{above}}$ for the surface current of Eq. (4-1) radiating in a homogeneous medium with parameters (μ, ϵ_2) . This result suggests that to a reasonable approximation $\underline{E}_{\text{en}}^{\text{C}}$ in region A can be taken as the electric field intensity radiated by $\underline{F}_{\text{en}}^{\text{C}}$ in a homogeneous medium with parameters (μ, ϵ_2) .

Next the problem of approximating E_{en}^C in region B will be considered. Figure 4-3 shows the electric field intensity in a rectangular dielectric cylinder illuminated at normal incidence by a plane wave. The ambient medium is free space with parameters (μ_0, ϵ_0) , and the cylinder has parameters $(\mu_0, 4\epsilon_0)$. The incident electric field intensity is one volt/meter. As seen in Fig. 4-3 the magnitude of the electric field in the cylinder varies from 1.08 to 1.12 volts/meter. Although not shown in Fig. 4-3, the phase of the electric field is essentially that of the incident wave. Thus roughly a 10% error would be incurred if the electric field in the slab were approximated by the incident field.

For field points in region B the approximation will be made that the electric field intensity radiated by an expansion mode is the field radiated by the expansion mode in the homogeneous medium (μ, ϵ) . It is felt that this is a reasonable approximation for electrically thin slabs whose density is not greatly different from that of the ambient medium, and for field points somewhat removed from the expansion mode.

In this section approximate expressions have been given for the fields of the expansion modes in the dielectric slab. The expressions given are not the most accurate available. They were chosen partly because they are simple and quickly evaluated on a digital computer.

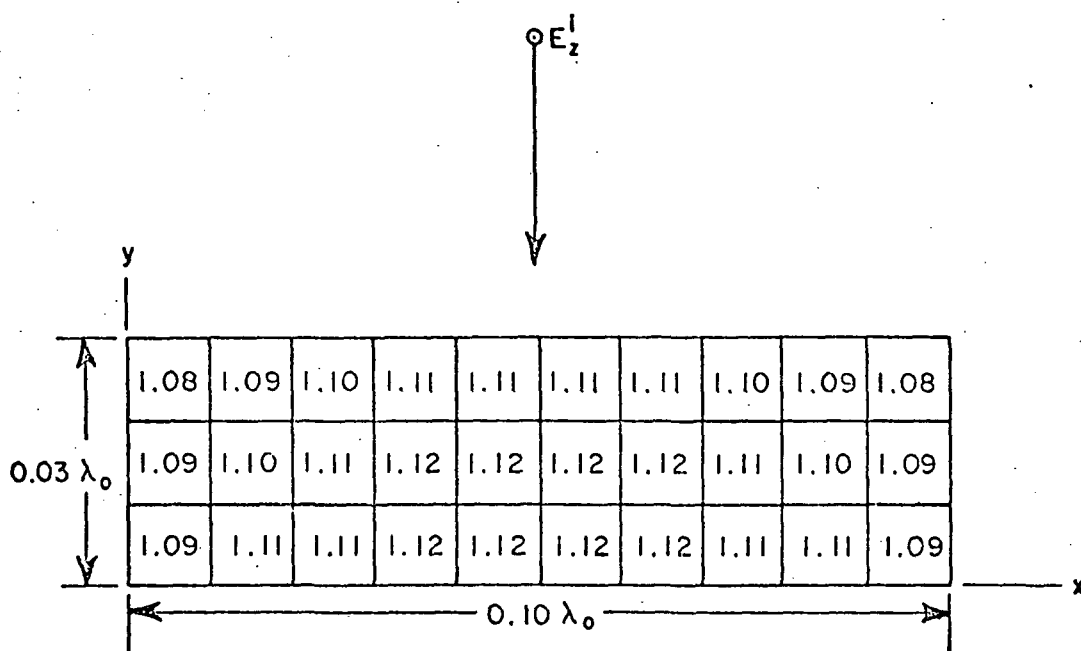


Fig. 4-3--Calculated electric field distribution in rectangular dielectric cylinder. The cylinder has infinite length, zero conductivity, $\epsilon = 4\epsilon_0$ and $\mu = \mu_0$. The incident field is a plane wave with normal incidence and unit electric field intensity. The bistatic scattering pattern is nearly circular. (This figure courtesy of J. H. Richmond.)

CHAPTER V STRIP ANTENNAS ARBITRARILY LOCATED IN A THIN DIELECTRIC SLAB

In the preceding chapters the problem of a strip antenna in the center of a thin dielectric slab was considered. The strips were restricted to be in the center of the slab so that symmetry could be used to proceed from Eq. (4-4) to Eq. (4-5). Figure 5-1 shows the end view of a dipole strip antenna located a distance d from the top surface of a slab of thickness T . The purpose of this section is to present approximate formulas for the impedance of strip antennas for $0 \leq d \leq T$. The strip antennas are restricted to be in a plane parallel to the top and bottom surfaces of the slab. An important special case of these formulas will be strip antennas on the surface of a thin dielectric slab ($d=0$). The methods presented in this chapter were suggested by Professor Ben Munk.

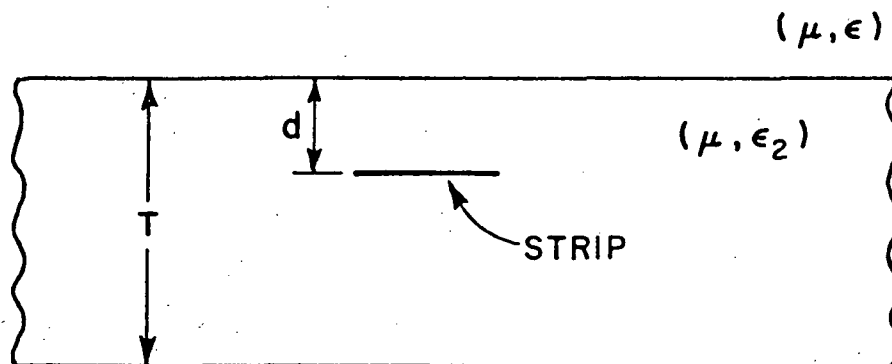


Fig. 5-1--The side view of a dipole located a distance d from the top surface of a dielectric slab of thickness T .

Figure 5-2a shows the side view of a strip dipole radiating in the homogeneous medium (μ, ϵ) . The impedance of this dipole can be thought of as being two impedances of equal value in parallel. The two impedances are the result of the antenna radiating to the left and to the right, and are equal from symmetry. Figure 5-2b shows the two impedances, each of value $2Z_0^0$, in parallel forming the antenna impedance Z_0^0 . The notation being used is that Z_d is the impedance of a strip antenna located a distance d from the top surface of a slab of thickness T (see Fig. 5-1).

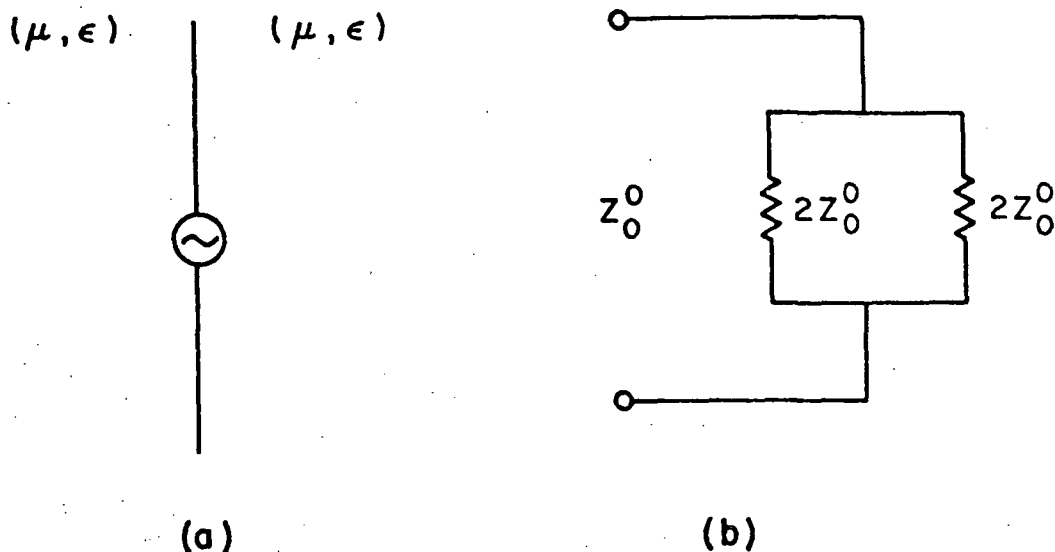


Fig. 5-2--(a) A strip dipole in a homogeneous medium and
(b) An equivalent circuit for its impedance.

Figure 5-3a shows the side view of a strip dipole in the center of a dielectric slab. Again the dipole impedance can be thought of as being two impedances in parallel. The two impedances are the result of the antenna radiating to the left and to the right, and are equal from symmetry. Figure 5-3b shows the two impedances, each of value $2Z_{T/2}^T$, in parallel forming the antenna impedance $Z_{T/2}^T$.

Finally, Fig. 5-4a shows the side view of a strip dipole off center in a dielectric slab. The antenna impedance is still thought of as the parallel combination of two impedances, but now the impedances are unequal. Referring to Fig. 5-4b the antenna input impedance, Z_d^T , is approximated by the parallel combination of $2Z_d^{2d}$ and $2Z_{T-d}^{2(T-d)}$:

$$(5-1) \quad Z_d^T = \frac{2Z_d^{2d} Z_{T-d}^{2(T-d)}}{Z_d^{2d} + Z_{T-d}^{2(T-d)}}$$

Z_d^{2d} and $Z_{T-d}^{2(T-d)}$ are the impedances of the antenna in the center of slabs of thickness $2d$ and $2(T-d)$ and can be evaluated using the methods of the preceding chapter.

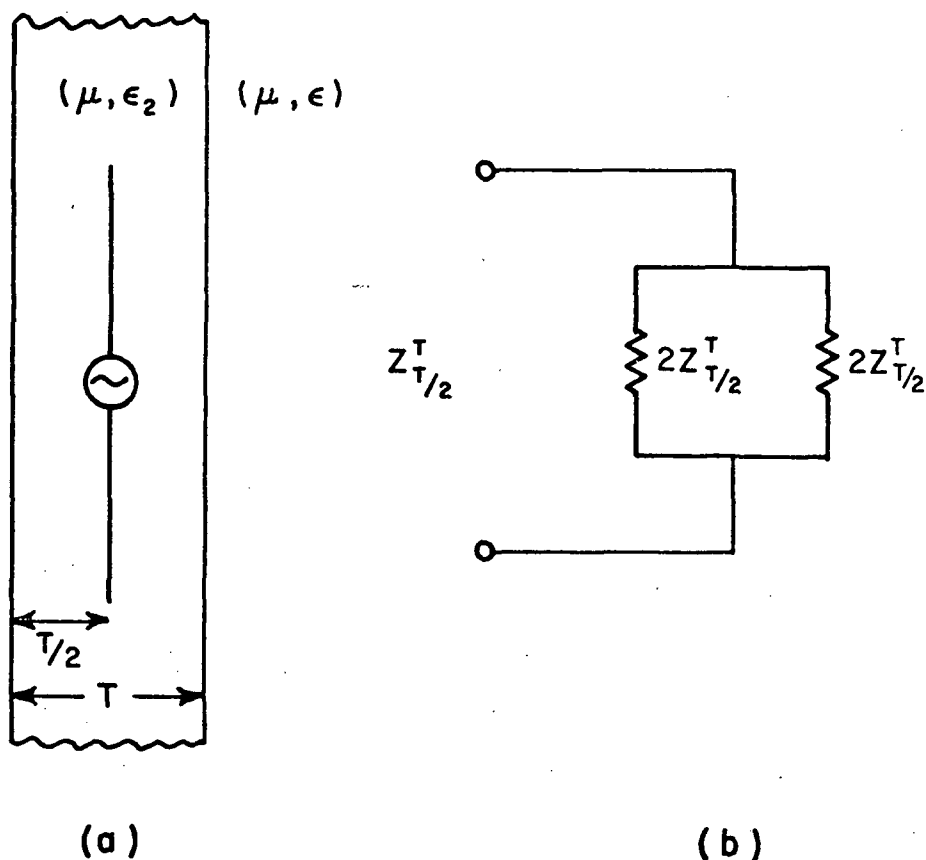


Fig. 5-3--(a) A strip dipole in the center of a dielectric slab and
(b) an equivalent circuit for its impedance.

Equation (5-1) is a relationship between the impedances of three different configurations. The conductor remains the same in all cases, but the location and thickness of the dielectric slab changes. For Eq. (5-1) to be a reasonable approximation the shape, but not magnitude, of the current distribution on all three antennas should be the same. This will be most nearly the case when the electrical lengths of the conductors are identical. In a homogeneous medium the electrical length is simply the physical length divided by the wavelength. However, an antenna in a dielectric slab is in an inhomogeneous medium, and the electrical length is not clearly defined. The definition of electrical length as a function of frequency for an antenna located a distance d from the top surface of a slab of thickness T will be taken as

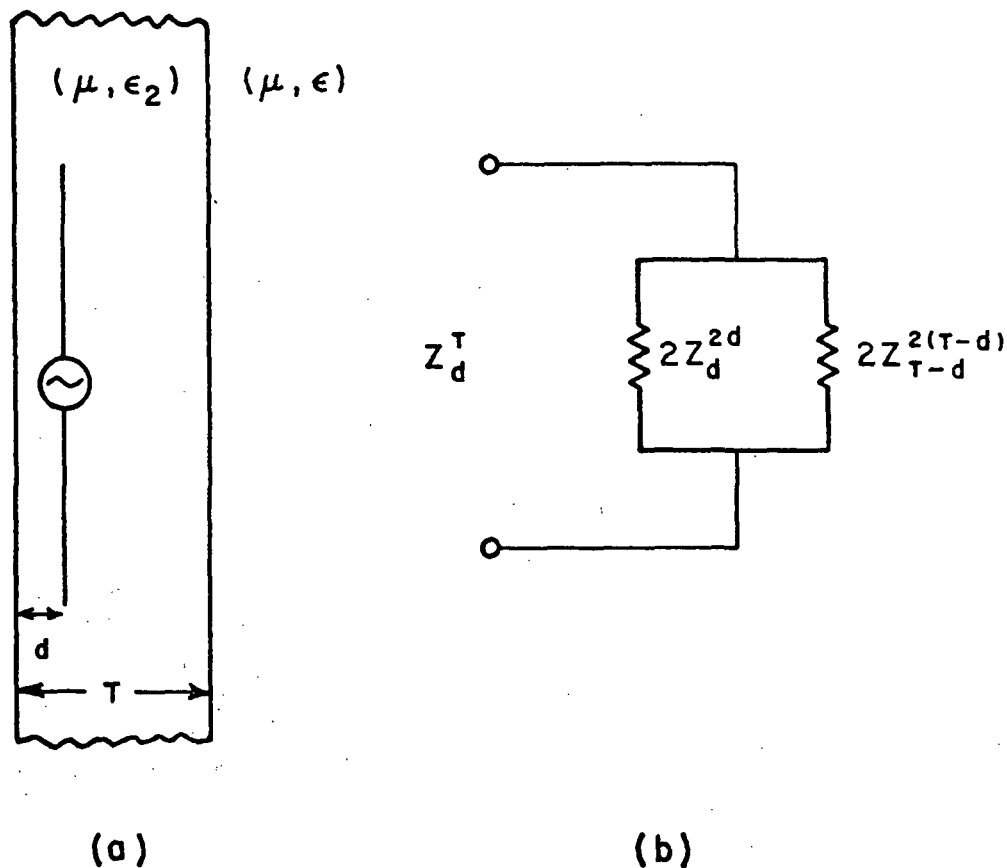


Fig. 5-4--(a) A strip dipole located off center in a dielectric slab and
 (b) an equivalent circuit for its impedance.

$$(5-2) \quad L_d^T(f) = \frac{\lambda(f)}{2R_d^T}.$$

Here $\lambda(f)$ is the electrical length of the antenna referred to the homogeneous medium exterior to the slab at the frequency f , and R_d^T is the electrical resonant length of the antenna located a distance d from the top surface of a slab of thickness T referred to the homogeneous exterior medium. According to this definition $L_d^T = 0.5$ at resonance.

The frequency dependence of Eq. (5-1) is now explicitly shown as

$$(5-3) \quad Z_d^T(f_1) = \frac{2 Z_d^{2d}(f_2) Z_{T-d}^{2(T-d)}(f_3)}{Z_d^{2d}(f_2) + Z_{T-d}^{2(T-d)}(f_3)}$$

with the understanding that f_1, f_2 , and f_3 are related by

$$(5-4) \quad L_d^T(f_1) = L_d^{2d}(f_2) = L_{T-d}^{2(T-d)}(f_3) .$$

Since $Z_d^{2d}(f)$ and $Z_{T-d}^{2(T-d)}(f)$ are considered to be known, R_d^{2d} and $R_{T-d}^{2(T-d)}$ are known, and $L_d^{2d}(f)$ and $L_{T-d}^{2(T-d)}(f)$ can be evaluated using Eq. (5-2). $L_d^T(f)$ is not known since R_d^T is not known. However, a reasonable approximation is

$$(5-5) \quad R_d^T = \frac{R_d^{2d} + R_{T-d}^{2(T-d)}}{2} .$$

An important special case of Eq. (5-3) is for the antenna on the surface of the slab in which case Eq. (5-3) becomes

$$(5-6) \quad Z_o^T(f_1) = \frac{2Z_o^0(f_2) Z_T^{2T}(f_3)}{Z_o^0(f_2) + Z_T^{2T}(f_3)} .$$

In the next chapter Eq. (5-6) will be used to evaluate the impedance of a strip dipole on the surface of a dielectric slab.

CHAPTER VI

NUMERICAL AND EXPERIMENTAL RESULTS

A. Introduction

In the preceding chapters equations are presented to analyze electrically thin strip antennas in or on an electrically thin dielectric slab. In this chapter numerical results based on these equations are compared with measurement and previously calculated results. In Chapter III, three methods are presented for treating antennas in the presence of a dielectric inhomogeneity. The calculations in this chapter are all based on the third method which is summarized by Eq. (3-27). All measurements were made at The Ohio State University ElectroScience Laboratory. As shown in Fig. 6-1 the measurements were made with strip monopoles in a dielectric slab. The monopoles were fed by a coaxial cable through a 2 ft. square groundplane with its edges terminating in 6 in. diameter cylinders to reduce edge reflections. The coaxial feed had an inner radius of $1/16$ in. and an outer radius of $3/8$ in.

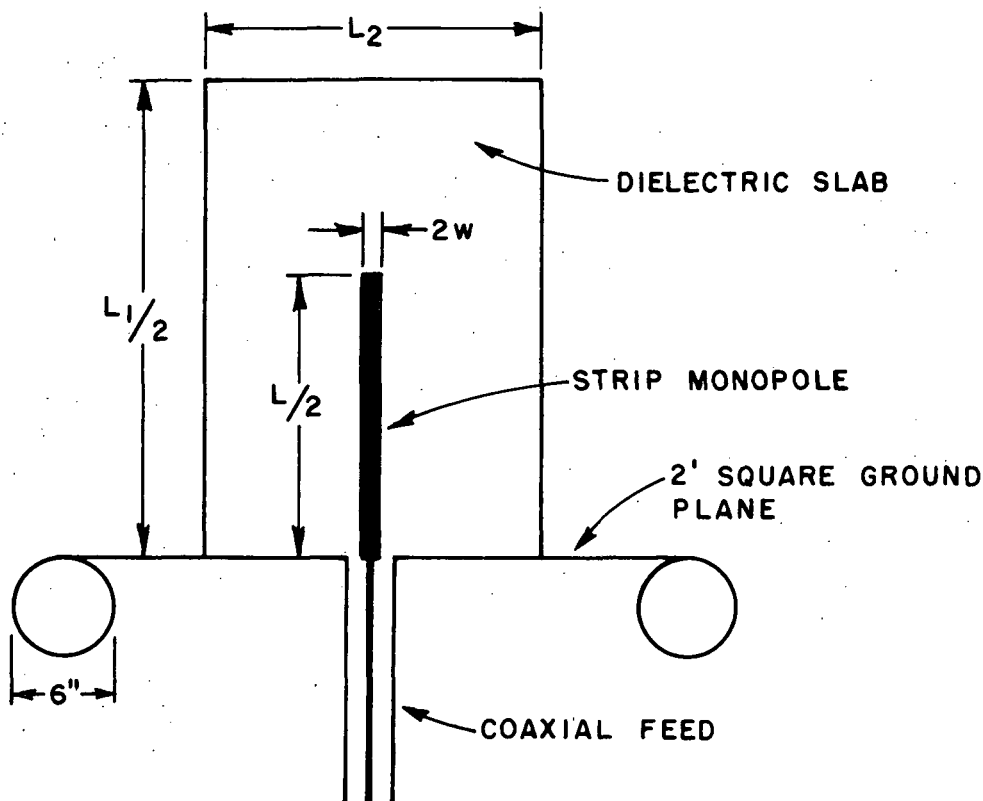


Fig. 6-1--Experimental arrangement for the measurement of the impedance of a strip monopole in a dielectric slab.

The numerical computations were made for a strip dipole symmetrically located in a dielectric slab as shown in Fig. 6-2. The dielectric slab is lossless, homogeneous, and isotropic. The dimensions of the broad faces of the slab are denoted L_1 and L_2 , and the slab thickness is denoted by T . The strip dipole has length L and width $2w$. It is center fed by a delta-gap generator and is located parallel to and at a distance d from the top surface of the slab. The slab has the permeability of free space and a permittivity ϵ_2 . All numerical data are for the dipole model.

B. Details of the Numerical Computations

Referring to Eq. (3-27), the computations required to determine the current on a strip antenna in the presence of a dielectric inhomogeneity can be grouped into four parts as follows:

1. Calculate the matrix Z .
2. Calculate the matrix Z and perform the matrix addition $Z + \Delta Z$.
3. Calculate the right hand side column V .
4. Solve the matrix Eq. (3-27) for the current column I .

Computer programs written by Richmond[19] and based on the piecewise-sinusoidal reaction formulation for electrically thin round wires in a homogeneous medium[10] are available and are capable of performing the computations illustrated by the flow graph of Fig. 6-3. A flow graph for a computer program based on the piecewise-sinusoidal reaction formulation for electrically thin strip wires in a dielectric slab is shown in Fig. 6-4. Comparing Figs. 6-3 and 6-4 shows that to treat the presence of dielectric inhomogeneity with Richmond's programs as a base, one needs only to calculate the matrix ΔZ , perform the matrix addition $Z + \Delta Z$, and store the result in the computer array which originally held the matrix Z . The steps outlined by the flow graph of Fig. 6-3 are described by Richmond.[19] Some of the details in the calculation of the matrix ΔZ will now be described.

The elements of the matrix ΔZ are given by the volume integration of Eq. (3-25). In this equation \underline{E}^m is the electric field intensity radiated by the m th sinusoidal test source in the homogeneous medium (μ, ϵ). As seen in Eq. (3-24), \underline{F}_{en}^p is proportional to \underline{E}_{en}^c , the electric field intensity radiated by the n th sinusoidal surface current expansion mode in the presence of the dielectric slab. The region of integration is the volume occupied by the dielectric slab. Simple closed form expressions and computer sub-routines exist to calculate \underline{E}^m . This author knows of no exact

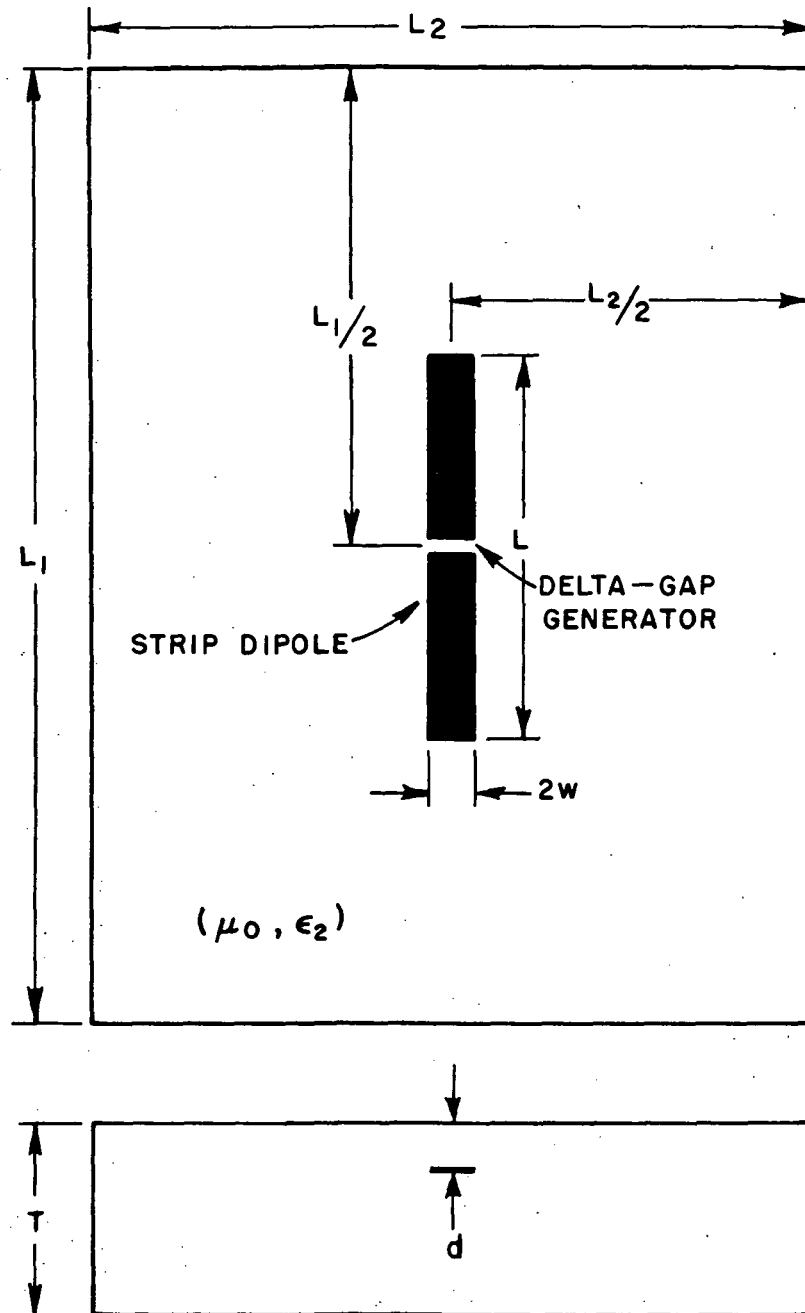


Fig. 6-2--A strip dipole in a finite dielectric slab.

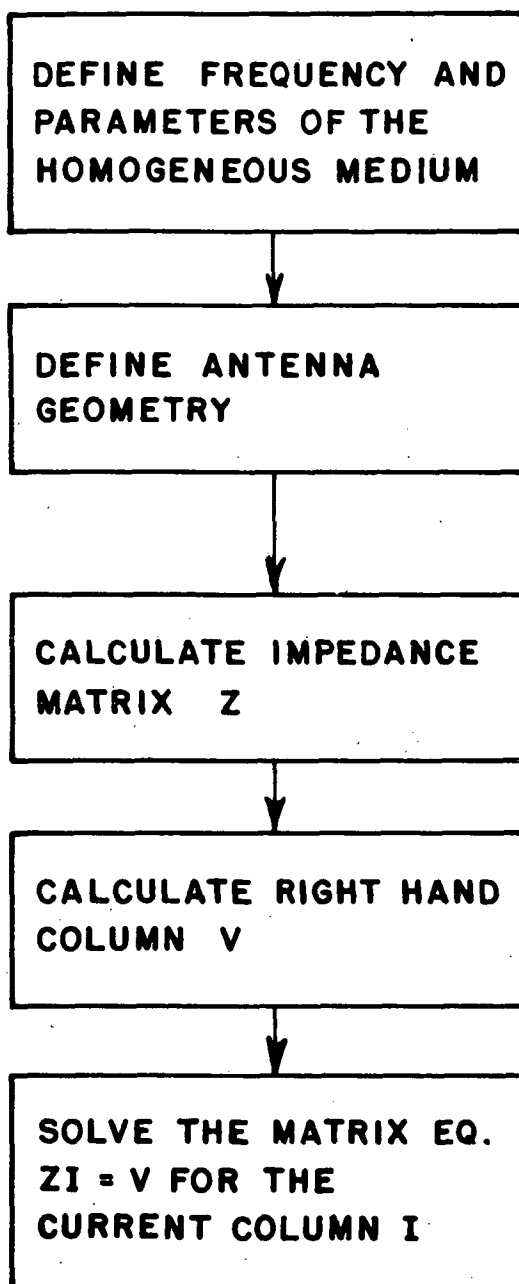


Fig. 6-3--A flow graph for a computer program for thin round wire antennas in a homogeneous medium.

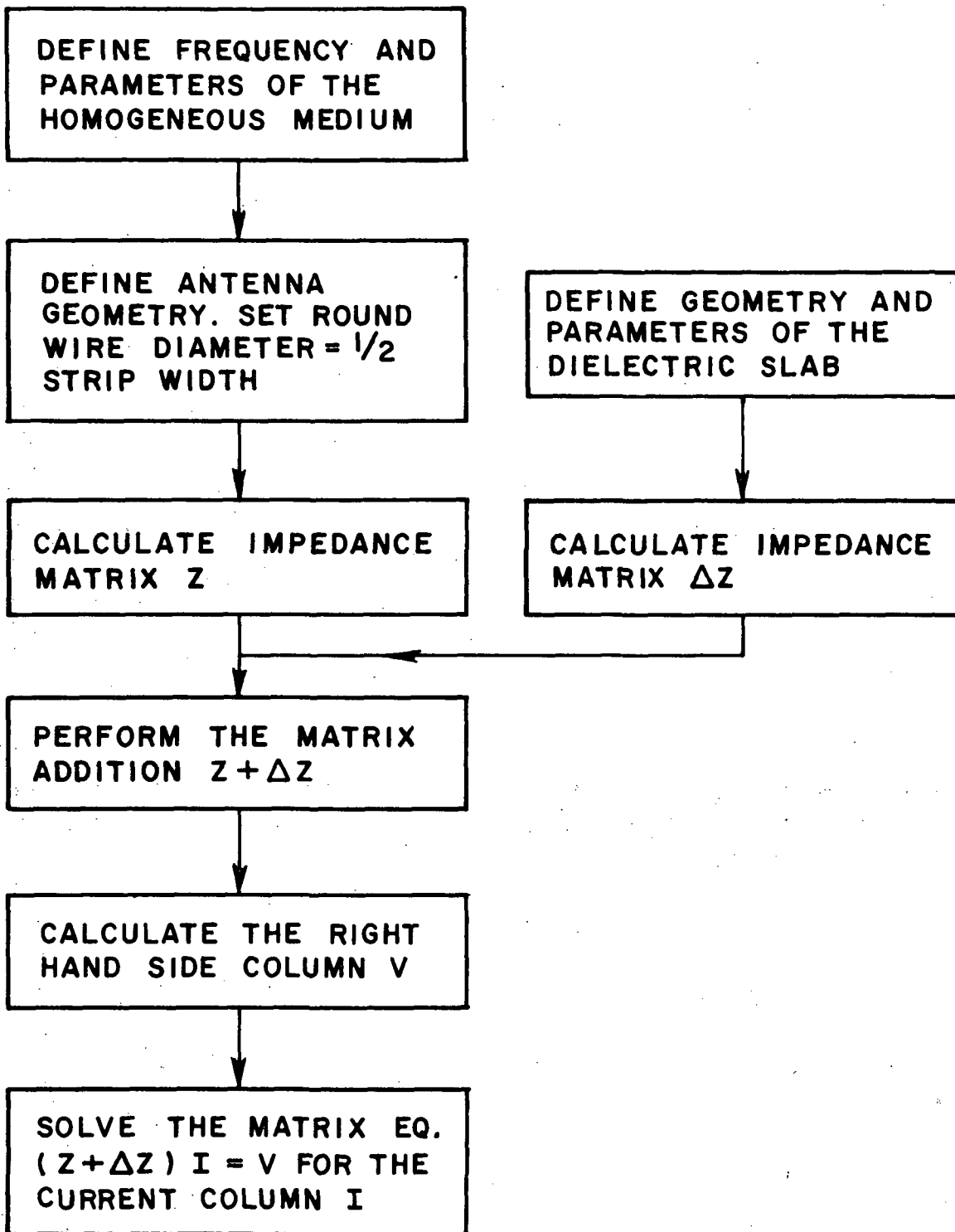


Fig. 6-4--A flow graph for a computer program for thin strip antennas in an inhomogeneous medium.

expressions for \underline{E}_{en}^C . However, in Chapter IV approximations for \underline{E}_{en}^C were presented. As shown in Fig. 4-2, the dielectric slab is divided into two regions which are denoted region A and region B. In the near zone region A, \underline{E}_{en}^C is approximated by the field of the nth expansion mode radiating in the homogeneous medium (μ, ϵ_2) . In the far zone region B, \underline{E}_{en}^C is approximated by the field of the nth expansion mode radiating in the homogeneous medium (μ, ϵ) . As seen in Fig. 4-2, the size of region A is defined by the parameter U_{\max} . Numerical experimentation has shown that a reasonable choice for U_{\max} is

$$(6-1) \quad U_{\max} = \begin{cases} \sqrt{w^2 + (T/2)^2} & \text{if } \sqrt{w^2 + (T/2)^2} \geq 1.2w \\ 1.2w & \text{if } \sqrt{w^2 + (T/2)^2} \leq 1.2w. \end{cases}$$

Since we are considering perfectly conducting strips, the \hat{z} components of the electric field should vanish at the strip surface, and also be small for field points very near the strip surface. It was found that with the approximations being used the \hat{z} components of \underline{F}_{en}^D and \underline{E}_{en}^M were both relatively large very near the conducting strip. This resulted in values for ΔZ_{mn} which were too large in magnitude to obtain good agreement between theory and experiment or previous results. This problem was overcome by setting the \hat{z} component of \underline{F}_{en}^D to zero for field points simultaneously in region B and in the region $|u| \leq w$ and $|z| \leq L/2$.

Referring to Fig. 6-2, for slabs with surface area $L_1 L_2$ on the order of a sixteenth of a square wavelength or more, the time required to perform the volume integration of Eq. (3-25) numerically will be on the order of minutes on a typical highspeed digital computer. If N expansion modes are being used, then depending on the amount of symmetry in a given problem, Eq. (3-25) will need to be evaluated between N and $(N^2+N)/2$ times to find the current on a given antenna at a given frequency. Clearly, prohibitive amounts of computer time could be required to make a calculation of impedance versus frequency. With the approximations being used, numerical results showed the elements of the ΔZ matrix to be almost pure imaginary (for a lossless dielectric) and also very nearly a linear function of frequency. In all of the plots of admittance versus L/λ to follow, the elements of the ΔZ matrix were calculated using Eq. (3-25) at $L/\lambda = 0.2$ and at $L/\lambda = 0.5$. Linear interpolation or extrapolation was then used to find ΔZ at other values of L/λ . This resulted in at least an order of magnitude reduction in computer time in making a plot of impedance versus frequency.

Before considering examples of dipoles in dielectric slabs, we will consider a dipole in free space. Figure 6-5 compares the calculated and measured admittance of a circular cross section copper dipole of length $L = 6"$, and radius $r = 0.025"$. The calculations were made by dividing the dipole into four equal segments. Referring to Eqs. (2-16) or (2-18), this resulted in three unknown piecewise sinusoidal expansion modes. Figure 6-5 shows good agreement between calculated and measured admittance. The discrepancies shown are partly due to experimental errors such as instrument calibration errors, room reflections, and reflections from the edges of the groundplane. At resonance ($f = 932$ MHz) the groundplane is about two wavelengths square. It was found that using more expansion modes in the theoretical calculations did not significantly improve the agreement between theory and experiment. When the dipole is put in a dielectric slab, the admittance will be perturbed by a larger amount than the difference between the calculated and measured results of Fig. 6-5. Thus, it is felt that the free space theoretical model and the measurements are sufficiently accurate to test the theory presented in Chapters III and IV.

Four examples will now be presented to demonstrate the ability of the theory to treat slabs of varying size. In these examples the dipole will be of length $L = 6$ in., width $2w = 0.1$ in., and in a slab of permittivity $\epsilon_2 = 2.55\epsilon_0$. The monopoles built for the experimental models were copper and approximately 0.003 in. thick. Figures 6-6 to 6-8 compare measured and calculated admittance for slabs of thickness 0.1 in. and of increasing size. Note that as the slab size increases, both experiment and theory predict that the resonant length decreases and the admittance level increases. Comparing Figs. 6-5 to 6-8 shows, as expected, that the dielectric closest to the antenna has the largest effect. Figure 6-9 shows the measured and calculated admittance for a slab identical to that of Fig. 6-8 except that the thickness T is increased to 0.256 in. Here it can be seen that increasing the slab thickness causes a considerable shift in resonant frequency and increase in the admittance level.

The next set of computations was made to compare with theoretical calculations made by Galejs.[8] Galejs calculated the impedance of a strip dipole in a plane stratified medium. He obtained a variational expression for the impedance in terms of infinite double integrals. Galejs did not make any quantitative comparisons between his results and measurements or previous calculations. His formulation is more general than the one presented here in the sense that he could treat electrically thin or thick slabs, or multilayered dielectrics. It is less general in the sense that it would be difficult to apply his method to antennas other than dipoles, and his method does not treat slabs of finite extent.

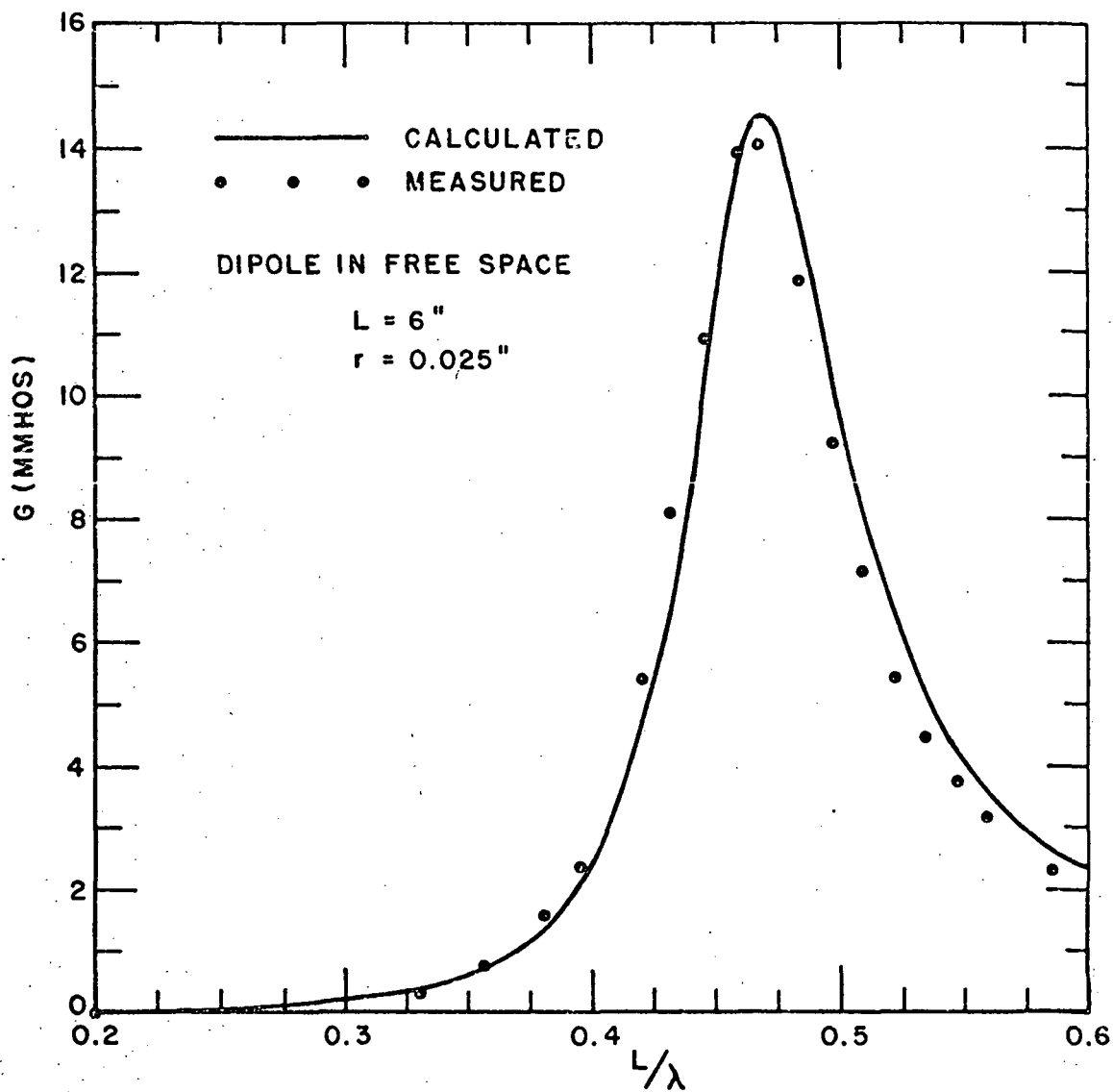


Fig. 6-5(a)--A comparison of calculated and measured conductance for a dipole in free space.

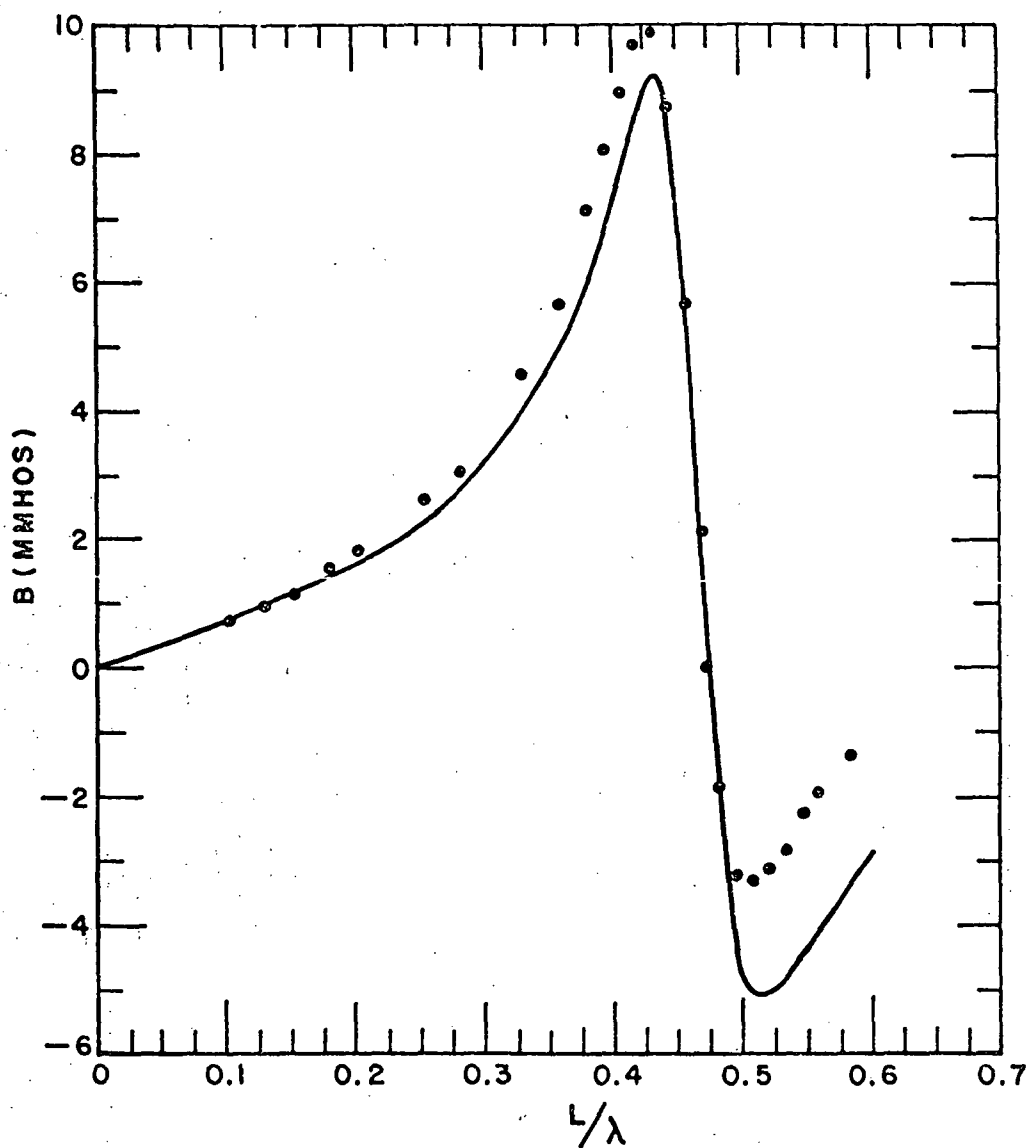


Fig. 6-5(b)--A comparison of calculated and measured susceptance for a dipole in free space.

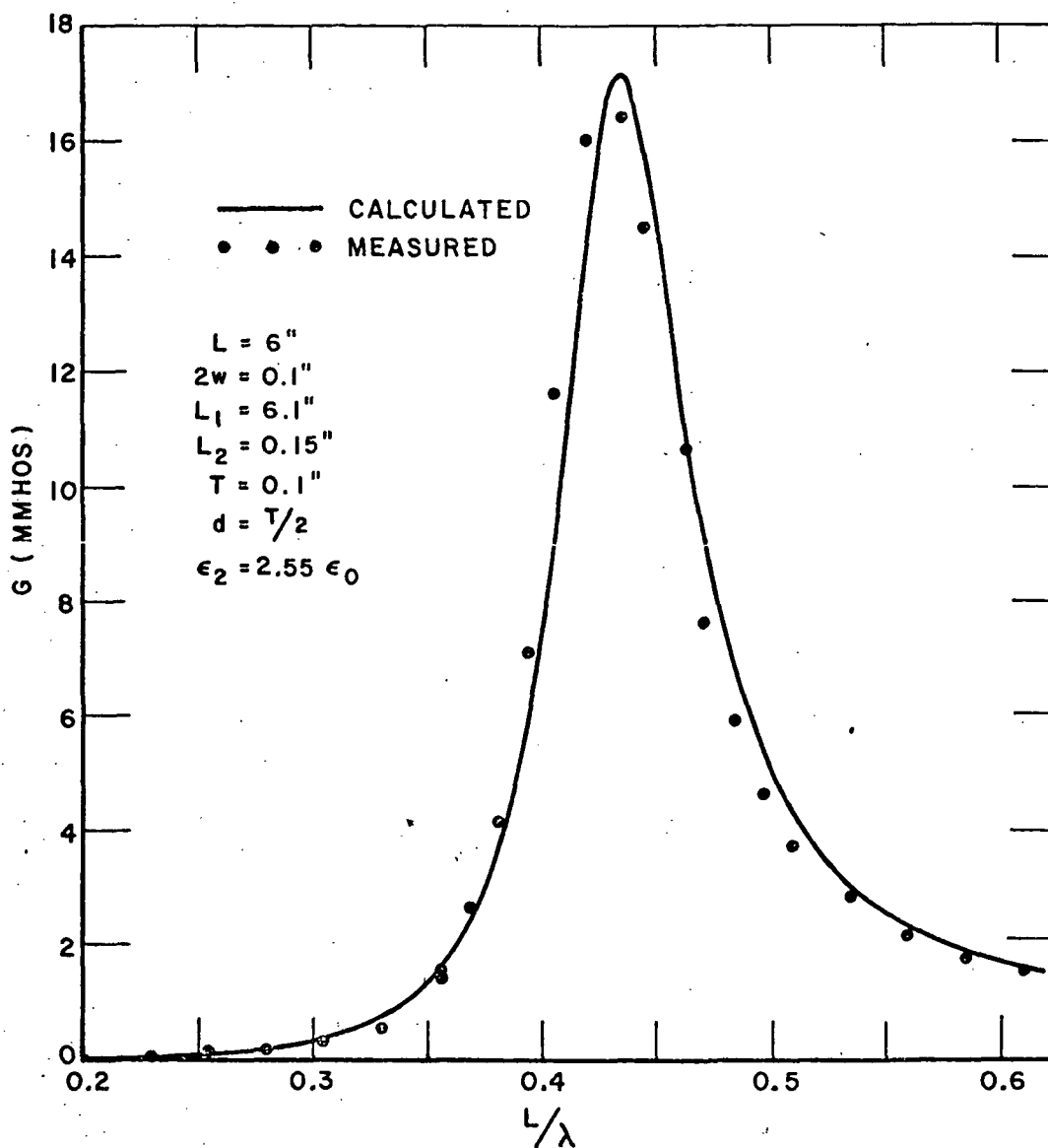


Fig. 6-6(a)--A comparison of calculated and measured conductance for a strip dipole in the center of a dielectric slab.

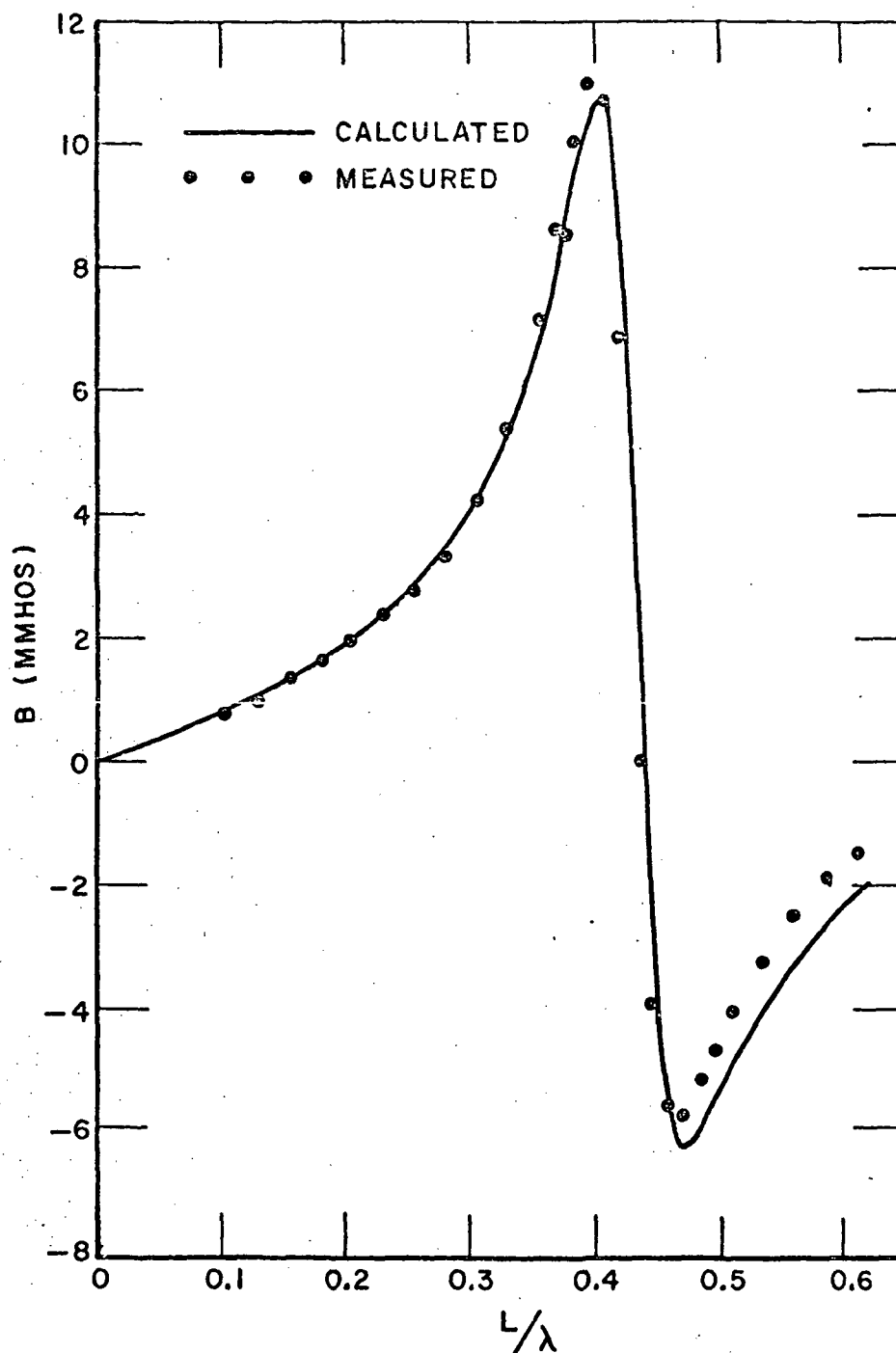


Fig. 6-6(b)--A comparison of calculated and measured susceptance for a strip dipole in the center of a dielectric slab.

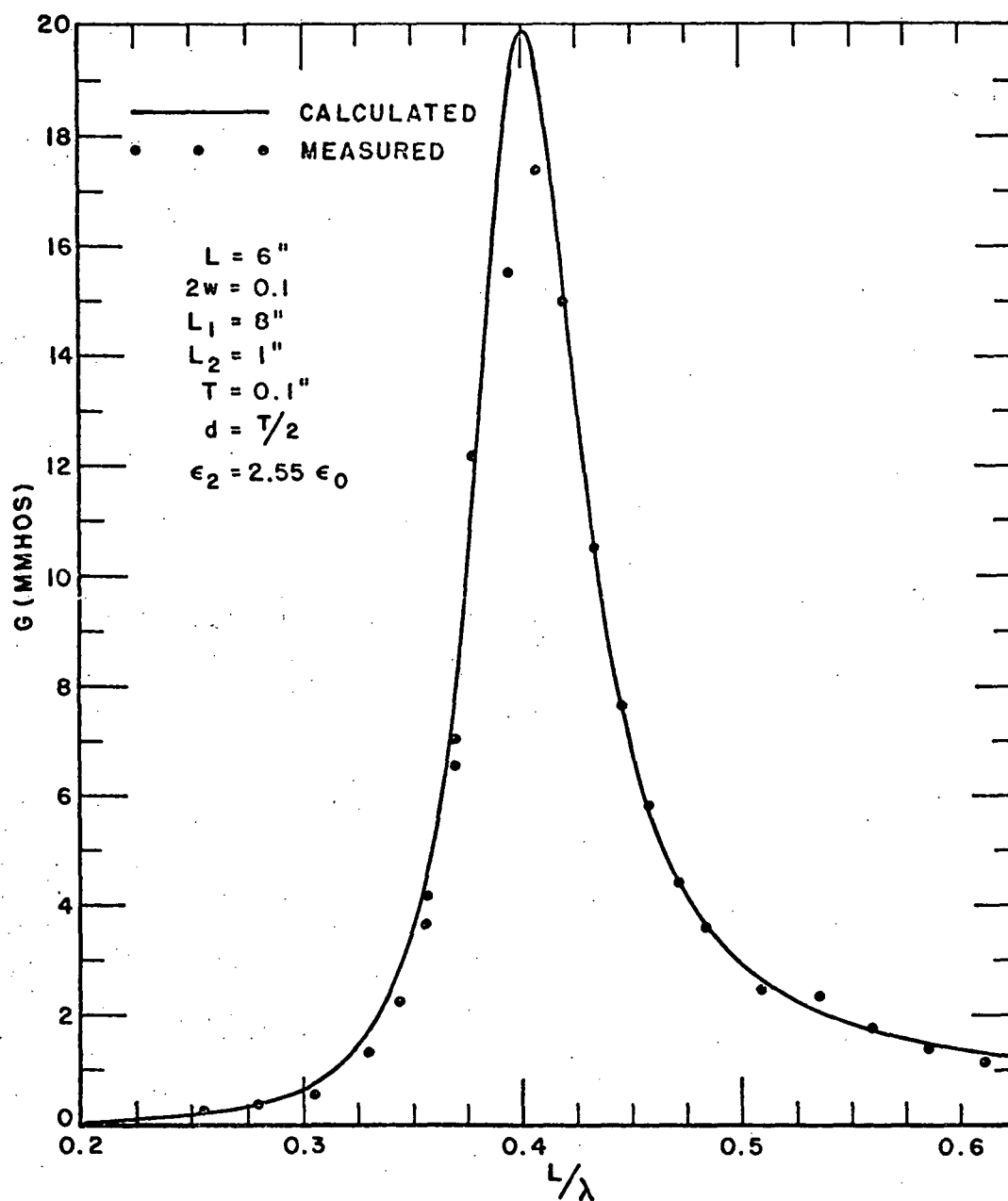


Fig. 6-7(a)--A comparison of calculated and measured conductance for a strip dipole in the center of a dielectric slab.

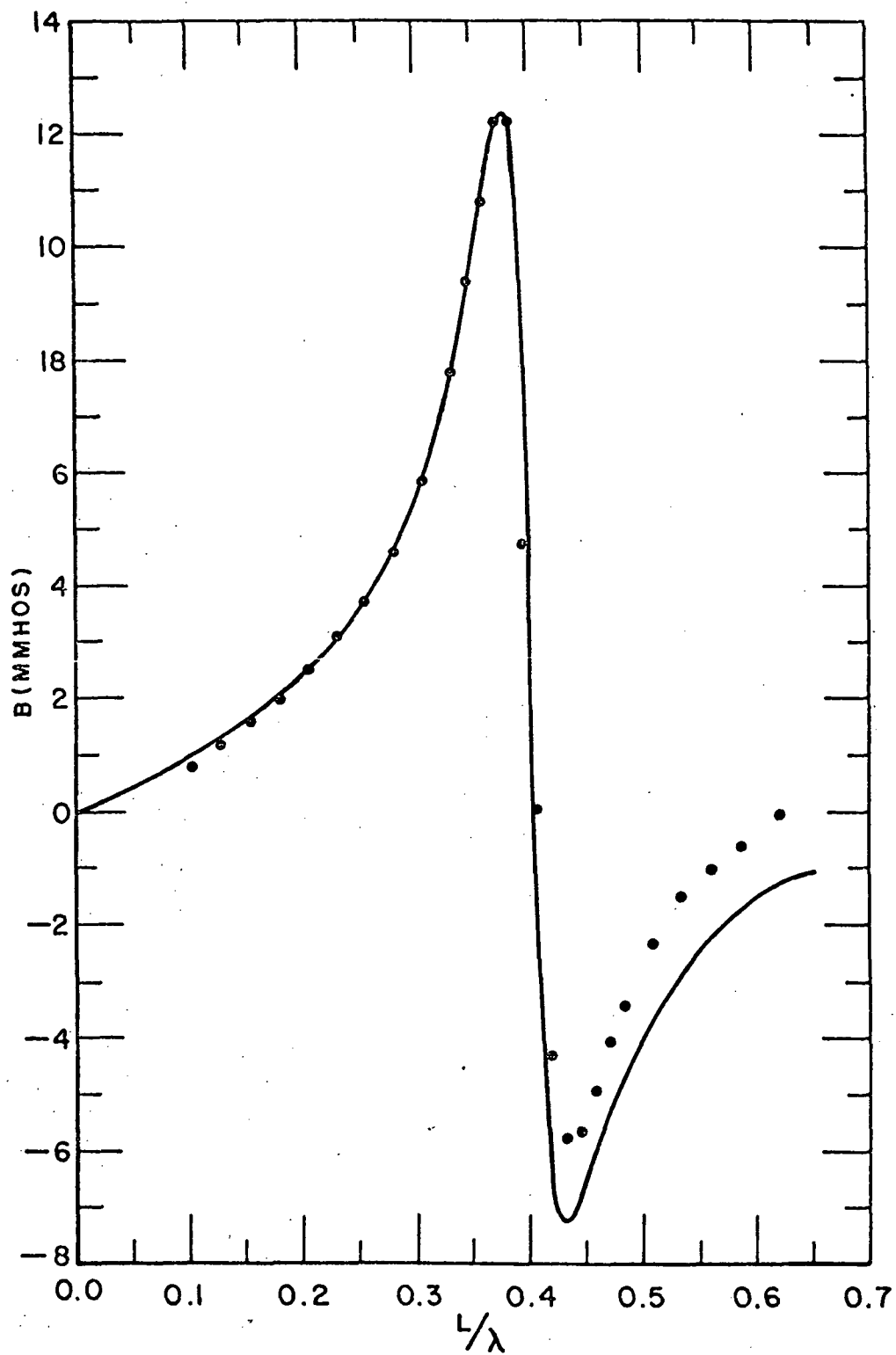


Fig. 6-7(b)--A comparison of calculated and measured susceptance for a strip dipole in the center of a dielectric slab.

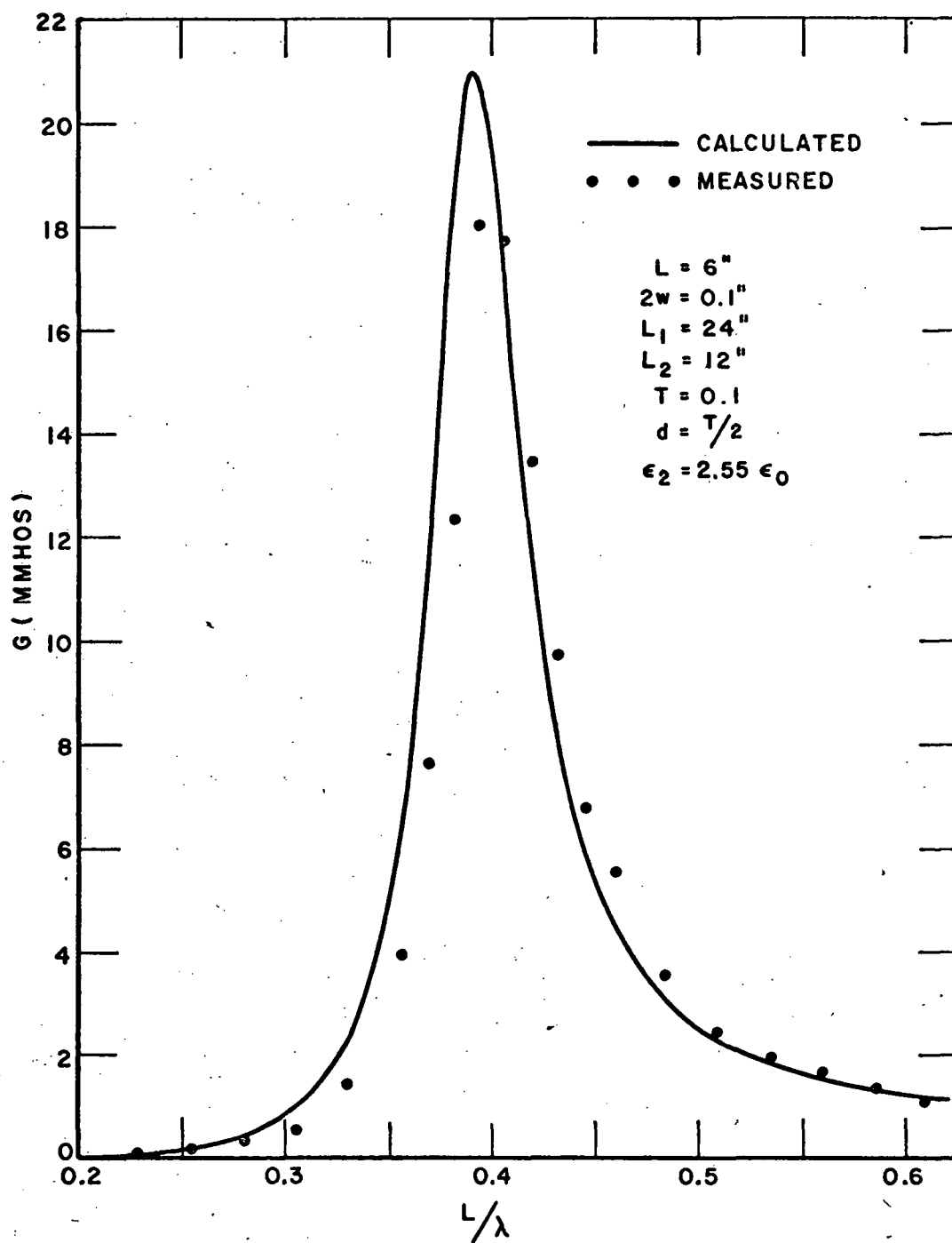


Fig. 6-8(a)--A comparison of calculated and measured conductance for a strip dipole in the center of a dielectric slab.

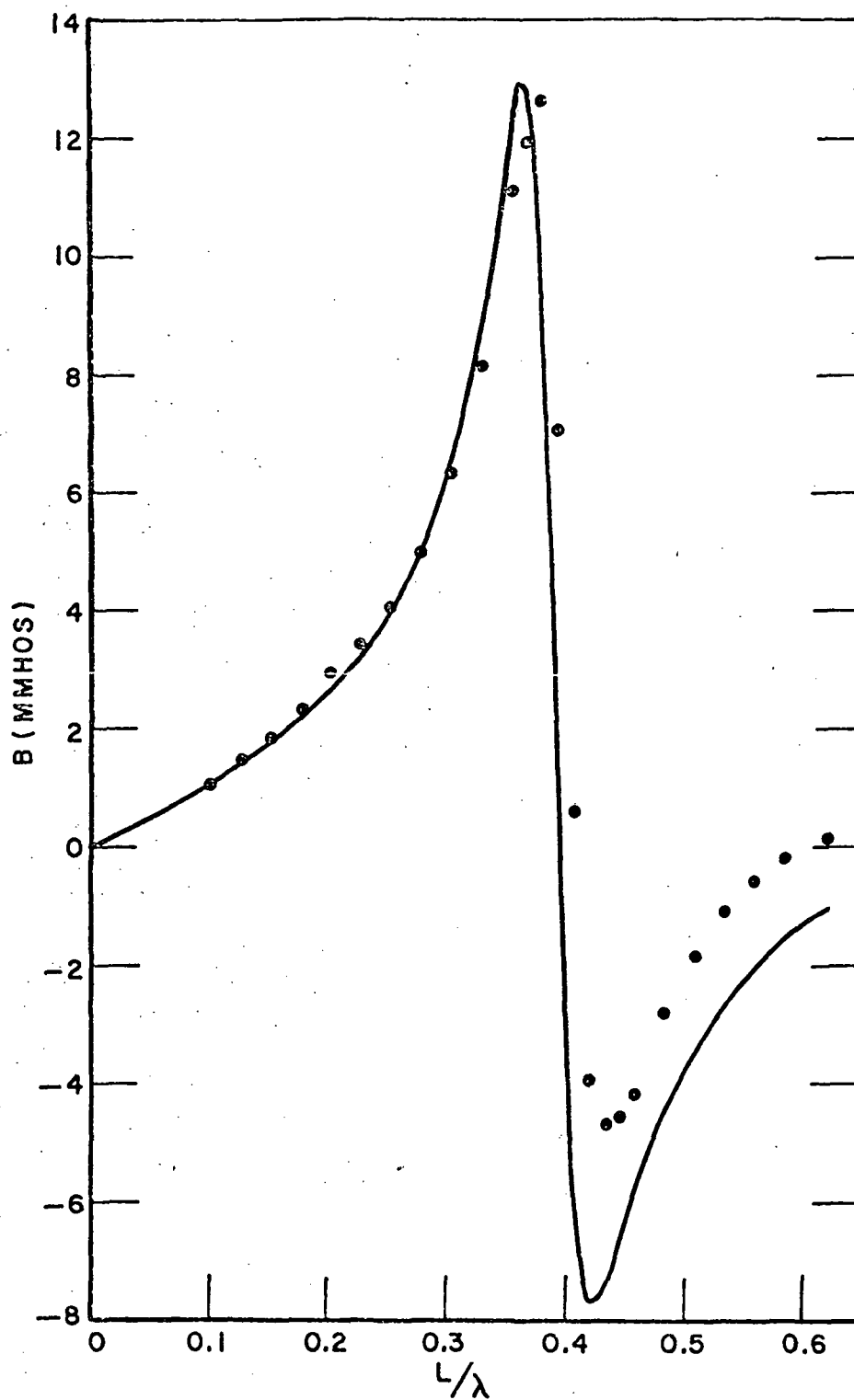


Fig. 6-8(b)--A comparison of calculated and measured susceptance for a strip dipole in the center of a dielectric slab.

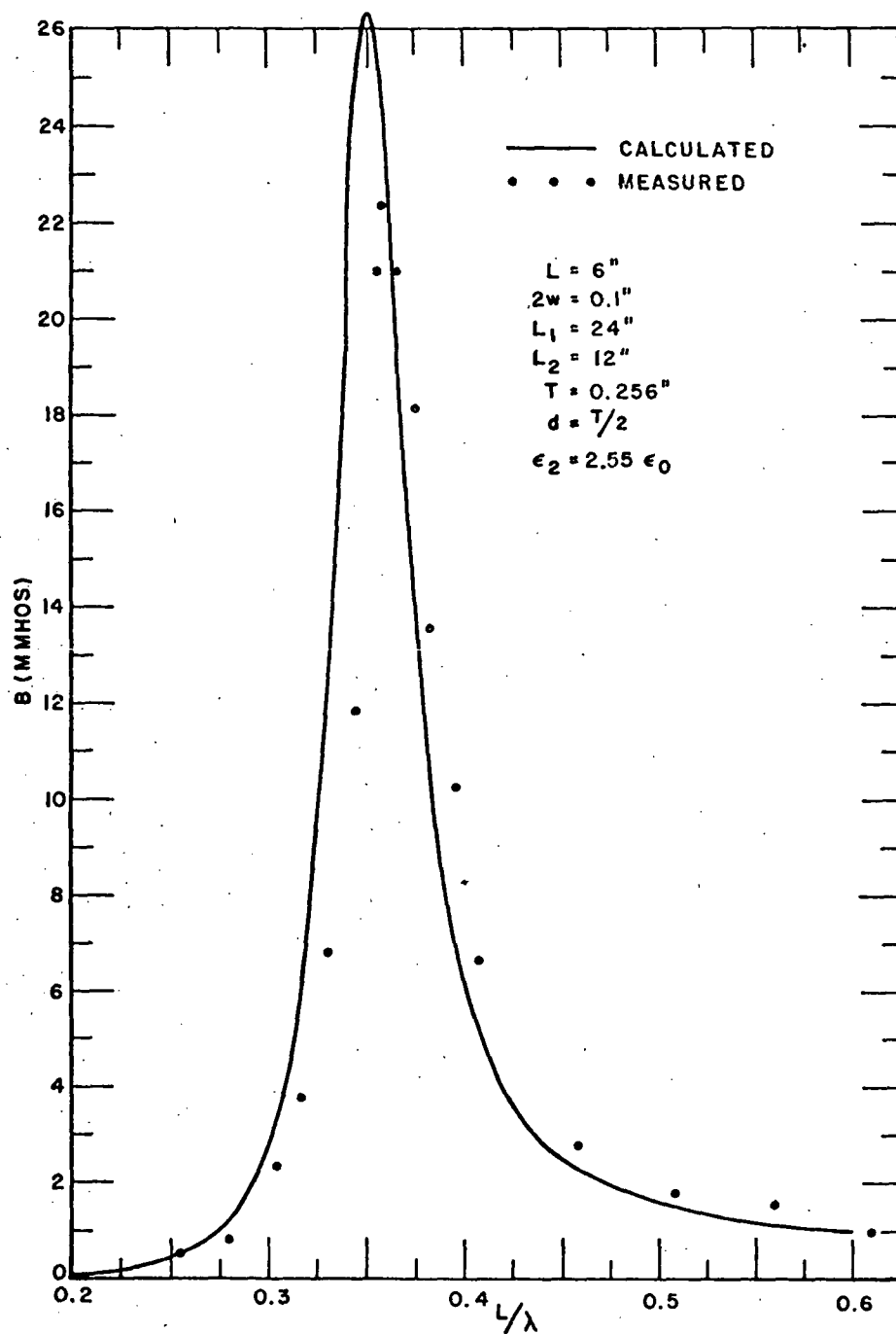


Fig. 6-9(a)--A comparison of calculated and measured conductance for a strip dipole in the center of a dielectric slab.

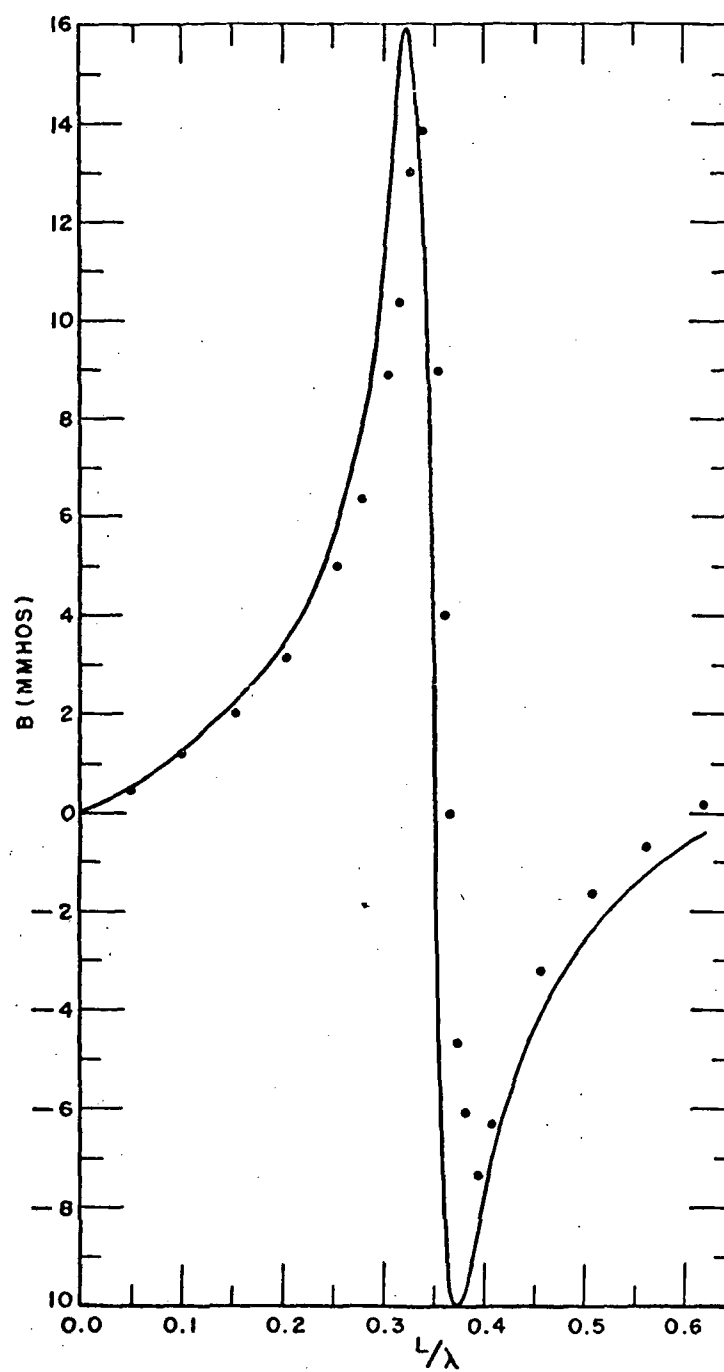


Fig. 6-9(b)--A comparison of calculated and measured susceptance for a strip dipole in the center of a dielectric slab.

Figures 6-10 to 6-12 compare the impedances of strip dipoles of various lengths in the center of a slab of thickness T and permittivity $\epsilon_2 = 2\epsilon_0$ as calculated by Galejs and the method presented here. In these figures

$$(6-2) \quad \Omega = 2 \ln (2L/w) = 8.$$

The present calculations were made for a lossless dielectric while Galejs' calculations were for a slab with loss tangent $\tan \delta = 0.03$. Figures 6-10 and 6-11 show that our calculations are in reasonable agreement with those of Galejs for slabs of thickness $T < 0.02\lambda$, and for dipoles of length $L = 0.4\lambda$ and 0.5λ . The agreement for the reactance worsens in Fig. 6-12 for the dipole of length $L = 0.6\lambda$. Note in Fig. 6-12 that the two solutions disagree even for slabs as thin as 0.002λ . Thus, the different reactances shown in Fig. 6-12 are probably a result of differences in the free space models.

As a final example we will consider a strip dipole on the surface of a slab of dimensions $L_1 = 24$ in., $L_2 = 12$ in., $T = 0.125$ in., and permittivity $\epsilon_2 = 2.55\epsilon_0$. The strip dipole is of length $L = 6$ in. and width $2w = 0.1$ in. The admittance of this dipole can be calculated using the data of Figs. 6-5, 6-9, and Eq. (5-6).^{*} Figure 6-13 shows reasonable agreement between theory and experiment for the strip dipole on the slab surface.

^{*}To use Eq. (5-6) the slab thickness should be 0.128 in. This discrepancy in thickness should cause little error.

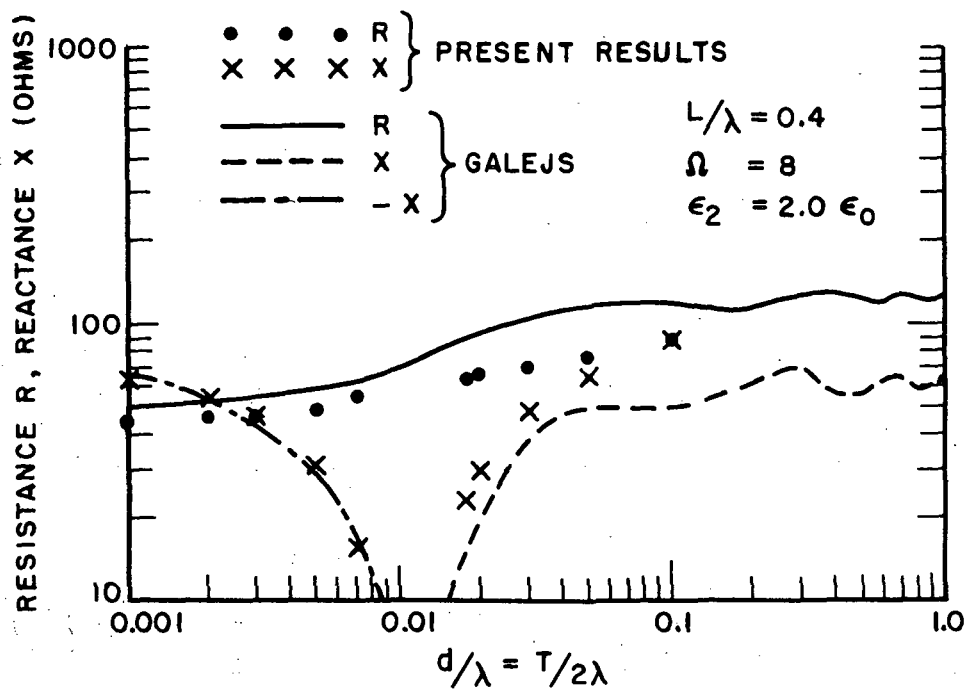


Fig. 6-10--A comparison of the present theory with a previous calculation for the impedance of a dipole of length $L = .4\lambda$ in the center of a dielectric slab.

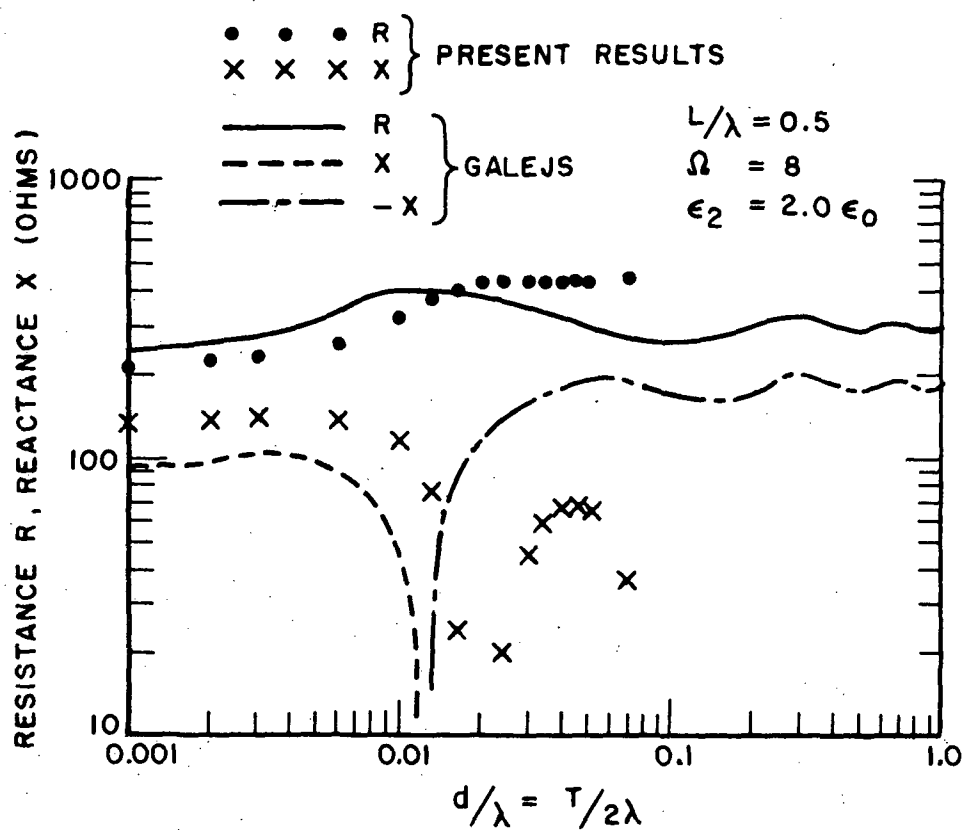


Fig. 6-11--A comparison of the present theory with a previous calculation for the impedance of a dipole of length $L = .5\lambda$ in the center of a dielectric slab.

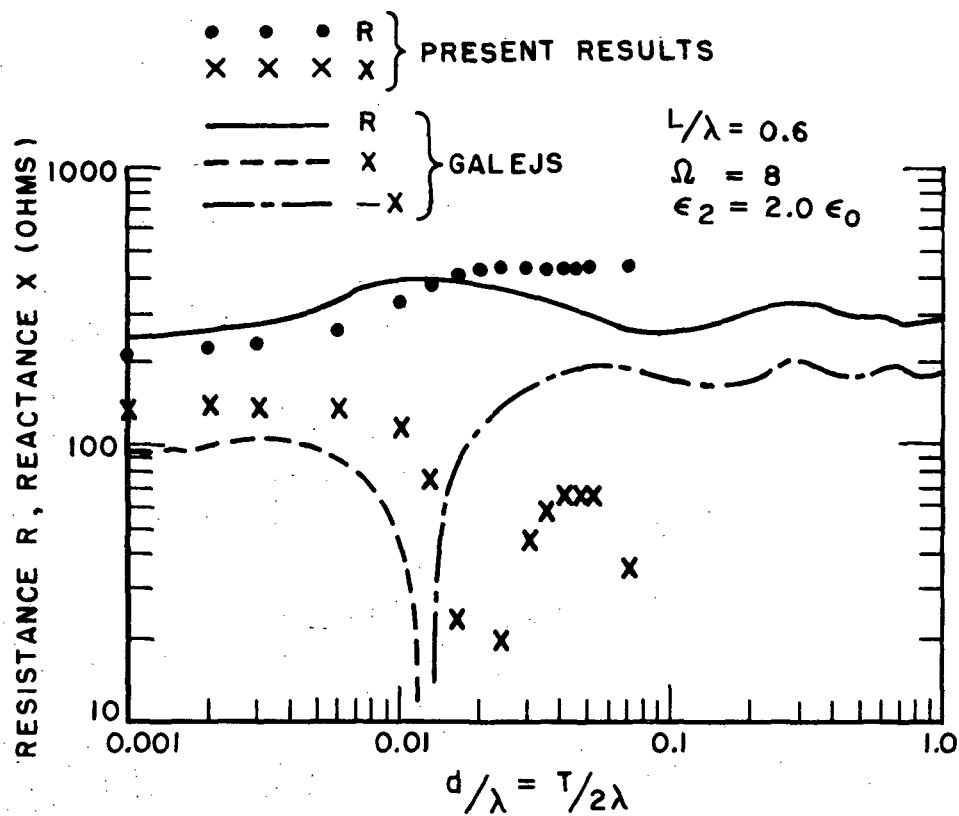


Fig. 6-12--A comparison of the present theory with a previous calculation for the impedance of a dipole of length $L = .6\lambda$ in the center of a dielectric slab.

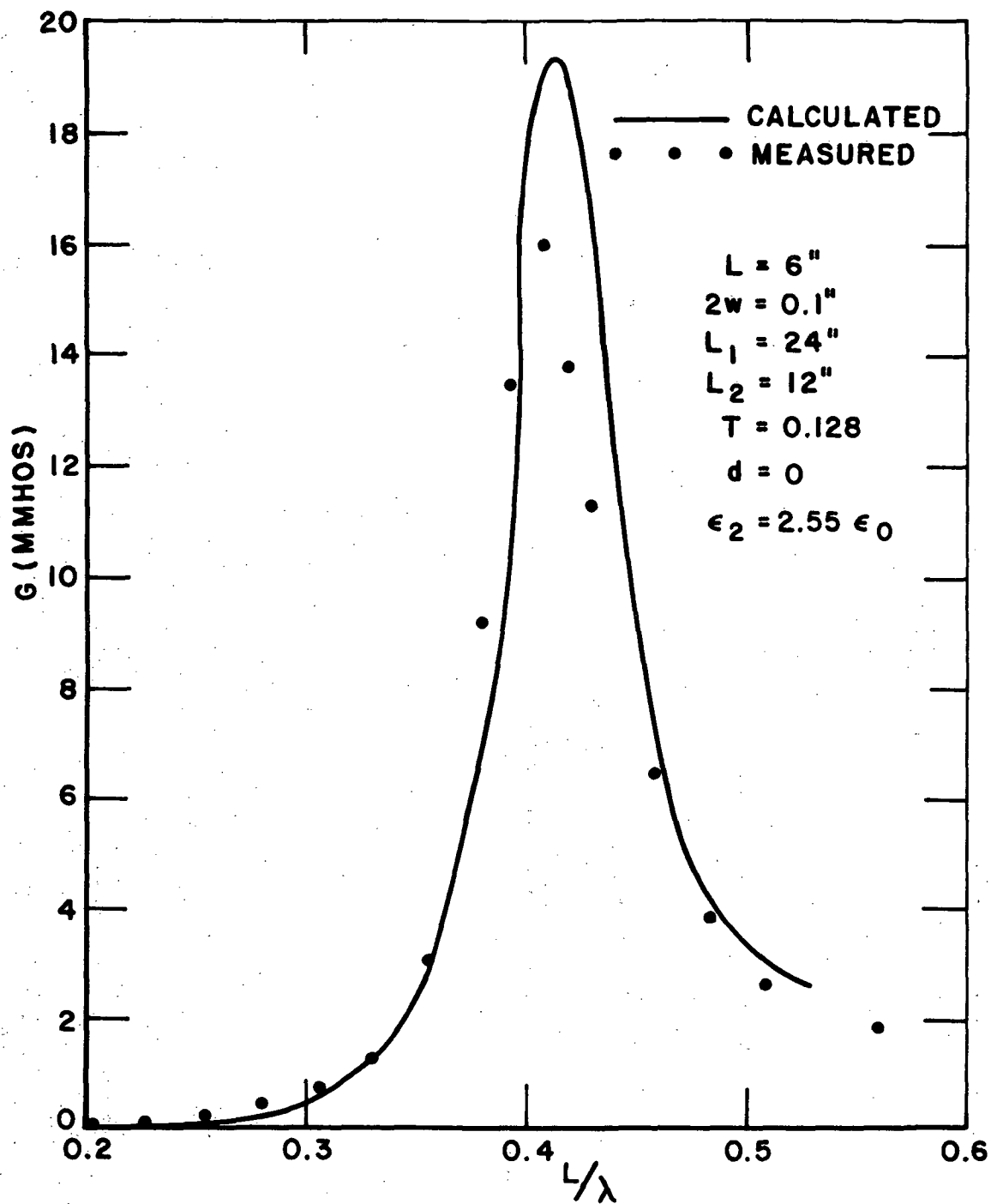


Fig. 6-13(a)--A comparison of calculated and measured conductance for a strip dipole on the surface of a dielectric slab.

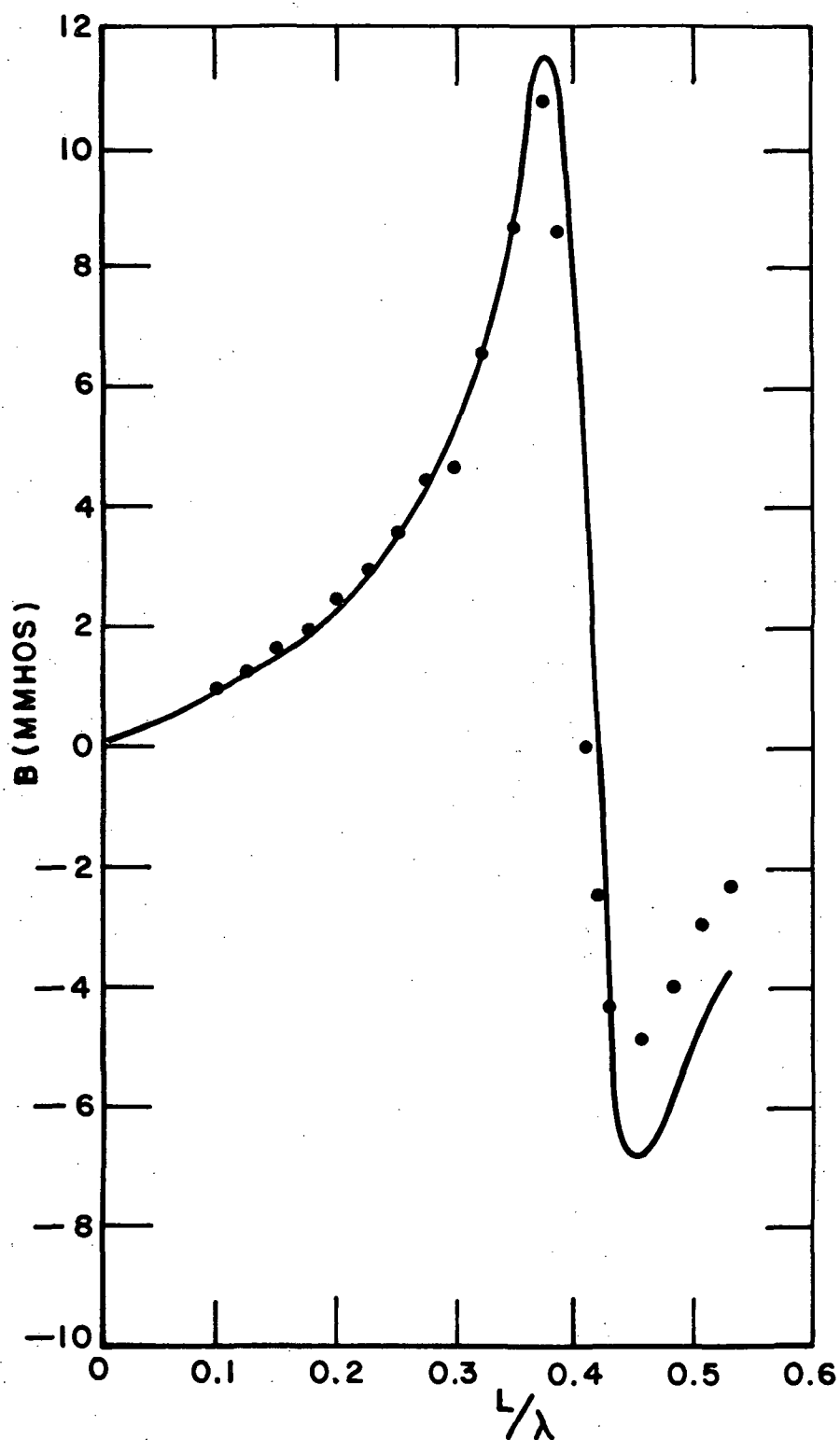


Fig. 6-13(b)--A comparison of calculated and measured susceptance for a strip dipole on the surface of a dielectric slab.

CHAPTER VII

CONCLUSIONS

The purpose of this study was to develop techniques to analyze electrically thin strip antennas in or on an electrically thin dielectric slab. The methods presented are moment method solutions and modifications of the piecewise sinusoidal reaction formulation for thin wire radiators in a homogeneous medium. The techniques are sufficiently general to be applicable to wire antennas in the presence of an arbitrary dielectric inhomogeneity.

The analysis was begun by considering thin strip antennas in a homogeneous medium. Next, three methods were presented for modifying the solution to account for the presence of an arbitrary dielectric inhomogeneity. In the first of these methods, the current on the wire and the electric field intensity in the inhomogeneity were considered to be independent unknowns. This method has the advantage of requiring a minimum of a priori knowledge concerning these fields, but has the disadvantage of requiring increased computer storage. For inhomogeneities which are not electrically small, this increase in computer storage can become prohibitive. In the last two methods, the current on the wire and the electric field in the inhomogeneity are considered to be dependent unknowns. These methods have the advantage of requiring very little additional computer storage, but have the disadvantage of requiring that a reasonable approximation to the fields radiated by a current element in the presence of the inhomogeneity be known. For the particular case of strip antennas in the center of an electrically thin dielectric slab, such approximations were presented for use with the third method. Thus, all numerical results presented are based on the third method. It was shown how to relate the impedance of a strip antenna in the center of a dielectric slab to its impedance off-center in the slab. An important special case was a strip antenna on the surface of a dielectric slab.

Numerical results were presented and compared with measurement and previous calculations. The numerical computations were restricted to dipole antennas, but the method is not limited to dipoles. These results showed the ability of the theory and the computer programs to calculate the impedance of strip dipoles in electrically thin dielectric slabs of varying thickness, length, and width.

It is felt that the solution can be improved by considering the currents on the wire and the fields in the dielectric to be dependent unknowns over most of the slab, but independent over a small volume of the slab. Referring to Fig. 4-2, this small volume might

be chosen between regions A and B. In this way one might hope to achieve increased accuracy and still be able to treat large slabs.

Using the general techniques presented here, for treating antennas in the presence of a dielectric inhomogeneity, one should be able to analyze the following problems:

1. Antennas or arrays of antennas printed on a dielectric slab.
2. An integrated radome and antenna system. This would require the analysis of strips printed on a curved dielectric substrate.
3. The microstrip antenna.[4,5] In analyzing the microstrip antenna, one might choose to represent the antenna using a surface patch rather than a wire-grid model.
4. Antennas in the presence of the human body. This is a problem of current interest and has applications to analyzing personal communication systems.

Also the techniques developed should be applicable to other problems involving dielectric inhomogeneities.

REFERENCES

- [1] Symposium on Microwave Strip Circuits, IRE Trans., Vol. MTT-3, (March 1955).
- [2] Munk, B. A., Kouyoumjian, R. G., and Peters, L., "Reflection Properties of Periodic Surfaces of Loaded Dipoles," IEEE Trans., Vol. AP-19, (September 1971), pp. 612-617.
- [3] Munk, B. A. and Luebbers, R. J., "Transmission Properties of Dielectric Coated Slot Arrays," Report 2989-8, February 1973, The Ohio State University ElectroScience Laboratory, Department of Electrical Engineering; prepared under Contract F33615-70-C-1439 for Air Force Avionics Laboratory, Wright-Patterson Air Force Base, Ohio. (AFAL-TR-73-26) (AD 907628L)
- [4] Howell, J. Q., "Microstrip Antennas," 1972 G-AP Symposium at the College of William and Mary, (December 1972), pp. 177-180.
- [5] Munson, R. E., "Conformal Microstrip Antennas and Microstrip Phased Arrays," IEEE Trans., Vol. AP-22, No. 1. (January 1974), pp. 74-78.
- [6] Bryant, T. G. and Weiss, J. A., "Parameters of Microstrip Transmission Lines and of Coupled Pairs of Microstrip Lines," IEEE Trans., Vol. MTT-16, (December 1968), pp. 1021-1027.
- [7] Yamashita, E. and Mittra, R., "Variational Method for the Analysis of Microstrip Lines," IEEE Trans., Vol. MTT-16, (April 1968), pp. 251-256.
- [8] Galejs, J., "Driving Point Impedance of Linear Antennas in the Presence of a Stratified Plasma," IEEE Trans., Vol. AP-13, (September 1965), pp. 725-736.
- [9] Harrington, R. F., Field Computations by Moment Methods, The Macmillan Co., New York, New York (1968).
- [10] Richmond, J. H., "Radiation and Scattering by Thin-Wire Structures in the Complex Frequency Domain," Report 2902-10, July 1973, The Ohio State University ElectroScience Laboratory, Department of Electrical Engineering; prepared under Grant No. NGL 36-008-138 for National Aeronautics and Space Administration.

- [11] King, R. W. P., The Theory of Linear Antennas, Cambridge, Mass., Harvard University Press, (1956), pp. 15-20.
- [12] Richmond, J. H., "The Basic Theory of Harmonic Fields, Antennas, and Scattering," unpublished notes, Chapter I.
- [13] Rumsey, V. H., "Reaction Concept in Electromagnetic Theory," *Physical Review*, Vol. 94, (June 15, 1954), pp. 1483-1491.
- [14] Richards, G. A., "Reaction Formulation and Numerical Results for Multiturn Loop Antennas and Arrays," Ph.D. Dissertation, The Ohio State University, 1970.
- [15] Agrawal, P. K., "Numerical Solution of Wire Antennas in a Cavity," Ph.D. Dissertation, The Ohio State University, 1972.
- [16] King, R. W. P., and Harrison, C. W., "Current Distribution and Impedance per Unit Length of a Thin Strip," *IEEE Trans.*, Vol. AP-14, (March 1966), p. 252.
- [17] Van Bladel, J., Electromagnetic Fields, New York, McGraw-Hill, (1964), pp. 382-387.
- [18] Richmond, J. H. and Geary, N. H., "Mutual Impedance of Nonplanar-Skew Sinusoidal Dipoles," Report 2902-18, August 1974, The Ohio State University ElectroScience Laboratory, Department of Electrical Engineering; prepared under Grant No. NGL 36-008-138 for National Aeronautics and Space Administration.
- [19] Richmond, J. H., "Computer Program for Thin-Wire Structures in a Homogeneous Conducting Medium," Report 2902-12, August 1973, The Ohio State University ElectroScience Laboratory, Department of Electrical Engineering; prepared under Grant No. NGL 36-008-138 for National Aeronautics and Space Administration.
- [20] Rhodes, D. R., "On the Theory of Scattering by Dielectric Bodies," Report 475-1, 1 July 1953, The Ohio State University ElectroScience Laboratory, Department of Electrical Engineering; prepared under Grant No. NGL 36-008-138 for National Aeronautics and Space Administration.
- [21] Richmond, J. H., "Scattering by a Dielectric Cylinder of Arbitrary Cross-Section Shape," *IEEE Trans.*, Vol. AP-13, (May 1965), pp. 334-341.

- [22] Richmond, J. H., "TE-Wave Scattering by a Dielectric Cylinder of Arbitrary Cross-Section Shape," IEEE Trans., Vol. AP-14, (July 1966), pp. 460-464.
- [23] Sommerfeld, A., "Über der Ausbreitung der Willen in der Drahtlosen Telegraphic," Ann. Physik., Vol. 28, (1909), pp. 663-737.
- [24] Sommerfeld, A., Partial Differential Equations in Physics, Academic Press, (1964), New York.
- [25] Banos, A., Dipole Radiation in the Presence of a Conducting Half-Space, Pergamon Press, (1966), New York.
- [26] Norton, K. A., "The Propagation of Radio Waves Over the Surface of the Earth and in the Upper Atmosphere. Part II. The Propagation from Vertical, Horizontal, and Loop Antennas Over a Plane Earth of Finite Conductivity," Proceeding of the Institute of Radio Engineers, Vol. 25, No. 9, Sept. (1937), pp. 1203-1236.
- [27] Miller, E.K., Poggio, A. J., Burke, G. J., and Selden, E. K., "Analysis of Wire Antennas in the Presence of a Conducting Half-Space: Part I. The Vertical Antennas in Free Space," Canadian Journal of Physics, Vol. 50, No. 9, May 1, 1972.